ROYAL SOCIETY OPEN SCIENCE

royalsocietypublishing.org/journal/rsos

Research

Cite this article: Hullot M, Martin C, Blondel C, Becker D, Rössner GE. 2024 Evolutionary palaeoecology of European rhinocerotids across the Oligocene–Miocene transition. *R. Soc. Open Sci.* **11**: 240987.
https://doi.org/10.1098/rsos.240987

Received: 5 July 2024
Accepted: 13 September 2024

Subject Category:
Earth and environmental science

Subject Areas:
palaeontology, evolution, ecology

Keywords:
Mi−1 event, dental wear, stable isotopes, enamel hypoplasia, body mass, diet

Author for correspondence:
Manon Hullot
e-mail: manon.hullot@gmail.com

Electronic supplementary material is available online at https://doi.org/10.6084/m9.figshare.c.7477982.

THE ROYAL SOCIETY PUBLISHING

Evolutionary palaeoecology of European rhinocerotids across the Oligocene–Miocene transition

Manon Hullot[1,2], Céline Martin[3], Cécile Blondel[4], Damien Becker[5,6] and Gertrud E. Rössner[1,7]

[1]Bayerische Staatssammlung für Paläontologie und Geologie, Staatliche Naturwissenschaftliche Sammlungen Bayerns, Munich 80333, Germany
[2]Centre de recherche en paléontologie Paris, Muséum national d'Histoire naturelle, CNRS, Sorbonne Université, Paris 75005, France
[3]Géosciences Montpellier, Université de Montpellier, CNRS, Montpellier 34090, France
[4]PALEVOPRIM Poitiers, Université de Poitiers, CNRS, Poitiers 86073, France
[5]JURASSICA Museum, University of Fribourg, Porrentruy 2900, Switzerland
[6]Department of Geosciences, University of Fribourg, Fribourg 1700, Switzerland
[7]Department für Geo- und Umweltwissenschaften, Paläontologie & Geobiologie, Ludwig-Maximilians-Universität München, Munich 80333, Germany

MH, 0000-0003-4147-9778; GER, 0000-0001-6538-5333

The Oligocene–Miocene transition witnessed great environmental and faunal changes, spanning from late Oligocene to early Miocene (MP28–MN3). Its drivers and consequences on mammals are, however, poorly understood. Rhinocerotoids are among the most affected taxa, reflected by great taxonomical and morphological changes. However, potential associated changes in ecology have not been explored. Here, we investigated the palaeoecology of 10 rhinocerotid species coming from 15 localities across Western Europe and ranging from MP28 to MN3. We explored evolutionary trends for diet, physiology and habitat via dental wear, hypoplasia, body mass and stable isotopy. All rhinocerotids studied were C3 feeders, whether browsing or mixed-feeding, but clear dietary differences were observed at some localities and between Oligocene and Miocene rhinocerotids. The prevalence of hypoplasia was low (less than 10%) to moderate (less than 20%), but there were great differences by loci, species and localities. Body mass covaried with hypoplasia prevalence, suggesting that larger species might be more susceptible to stresses and environmental changes. We reconstructed similar warm conditions at all localities except Gaimersheim, but found greater variations in precipitation. Indeed, a clear shift in $\delta^{13}C$ values was noticed

at the end of the Oligocene, consistent with climatic and vegetation changes reported at that time.

1. Introduction

While the Oligocene–Miocene transition (OMt) also marks the boundary between two periods (Palaeogene and Neogene), this event has received little attention; hence, its drivers and consequences on terrestrial faunas remain poorly understood [1]. Despite the apparent global climatic stability reconstructed during the Oligocene and Early Miocene (coolhouse episode: 34–15 Ma), major punctual (spatially and/or temporally) climatic fluctuations occurred during this interval, including the Late Oligocene Warming (26.5–24.5 Ma) and the Mi−1 glaciation event (23.28–22.88 Ma) [2,3]. The Late Oligocene Warming occurred between the Mammal Palaeogene reference level (MP) 26 and MP28 [3], and was responsible for a temperature increase in terrestrial environments of up to 10°C [4–6]. The Mi−1 event is one of the three largest climatic aberrations of the Cenozoic, occurring at the Oligocene–Miocene boundary and responsible for a prolonged cooling lasting about 400 kyr [7–9]. Both events might have critically impacted the food resources and habitats, which might be reflected in the palaeoecological preferences of the fauna.

A few studies have investigated mammal occurrence during the OMt and yielded contrasting results. Micro-mammal occurrences point towards a relative faunal homogeneity across Europe with no particular changes in communities at the Oligocene–Miocene boundary [1,10]. The trend is very different for large herbivore mammals, for which Scherler *et al*. [11] described a three-phased transition of the assemblages (genus and family levels) over a long period of time from the MP28 to the Mammal Neogene zone (MN) 3. Moreover, some faunal changes are reported during the OMt, as classical components of Palaeogene faunas disappear. This is notably the case of 'hyracodontid' and amynodontid rhinocerotoids, leaving only one family of rhinoceroses from the Miocene onward: the Rhinocerotidae or true rhinoceroses.

The super-family of Rhinocerotoidea—including Eggysodontidae, Paraceratheriidae, Amynodontidae and Rhinocerotidae—is the most abundant and diversified within the Perissodactyla [12]. More than 300 species are recognized from the Eocene onward in various terrestrial ecosystems of all continents but Antarctica and South America [13]. Rhinocerotidae arrived in Europe after the *Grande Coupure* (early Oligocene), but only reached their peak of alpha-diversity shortly after the OMt (Burdigalian) [14], with often several co-occuring species documented in the Neogene faunas. Today, rhinoceroses are the largest herbivore species with both grazing and browsing preferences [15], and the past diversity could have been even greater, as evident changes in locomotion and dental morphology are documented throughout the evolutionary history of this family [11,14]. However, rhinocerotids' palaeoecology has rarely been explored.

Here, we investigate the palaeoecology of 10 rhinocerotid species coming from 15 localities across Western and Central Europe covering the Oligocene–Miocene transition interval (MP28–MN3). As climatic events might have impacted food resources and habitats, and as morphological changes have already been noted for rhinocerotids during the OMt [11], we expect to detect changes in the palaeobiology and palaeoecology of these taxa as well. We explore evolutionary trends for body mass (dental measurements), dietary preferences (dental wear and carbon isotopes) and stress susceptibility (enamel hypoplasia) to infer the palaeoecological niche and its spatio-temporal evolution. This approach allows discussion of some aspects of niche partitioning or competition, and provides new palaeoenvironmental insights (mean annual temperature and precipitation) at several localities. We anticipate a shift in dietary preferences between Oligocene and Miocene rhinocerotids and an increase of body mass during the earliest Miocene associated with the appearance of mediportal forms.

2. Material and methods

We studied approximately 1800 teeth of rhinocerotids (see all details in electronic supplementary material, S1) from 15 European localities dating to the OMt (MP28–MN3; figure 1 and details on localities in electronic supplementary material, S2). The specimens are curated at the following institutions: Bayerische Staatssammlung für Paläontologie und Geologie Munich (Gaimersheim, Pappenheim, Wintershof-West), Centre d'étude et de Conservation du Muséum Marseille (Paulhiac,

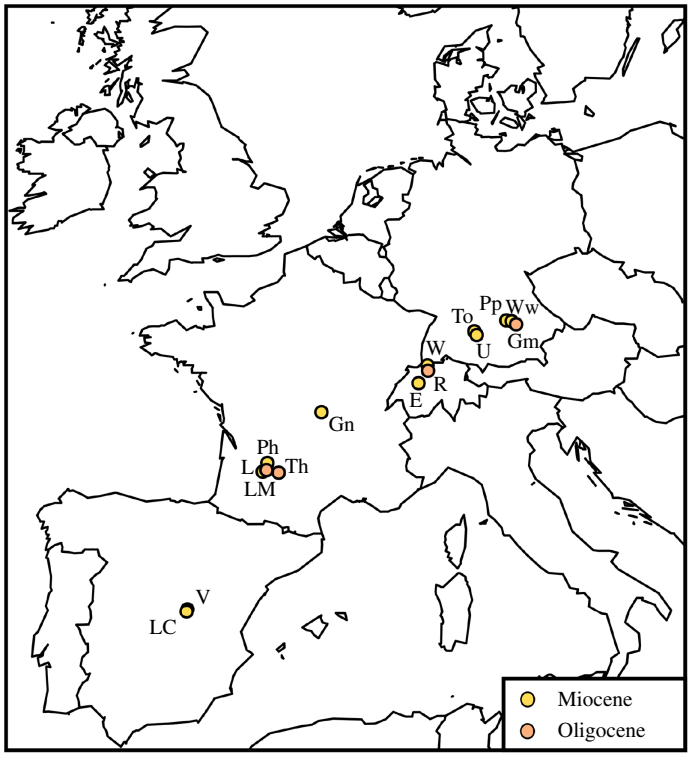

Figure 1. Localization of the studied localities in Central and Western Europe. Abbreviations: E, Engehalde (MN2); Gm, Gaimersheim (MP28); Gn, Gannat (MP30-MN1); L, Laugnac (MN2, reference); LC, Loranca del Campo (MN3a); LM, La Milloque (MP29); Ph, Paulhiac (MN1, reference); Pp, Pappenheim (MN2); R, Rickenbach (MP29; reference), To, Tomerdingen (MN1); Th, Thézels (MP30); U, Ulm-Westtangente (MN2a); V, Valquemado (MN2); W, Wischberg (MN1); and Ww, Wintershof-West (MN3).

Laugnac), Musée des Confluences de Lyon (Gannat), Museo Nacional de Ciencias Naturales Madrid (Loranca del Campo, Valquemado), Museum National d'Histoire Naturelle Paris (Gannat, La Milloque, Thézels), Naturhistorisches Museum Basel (Gannat, La Milloque, Laugnac, Paulhiac, Thézels, Rickenbach), Naturhistorisches Museum Bern (Engehalde, Wischberg), Naturmuseum Olten (Rickenbach), Rhinopolis (Gannat, deposited at Paleopolis), Staatliches Museum für Naturkunde Stuttgart (Tomerdingen, Ulm-Westtangente), University Claude Bernard Lyon 1 (Laugnac, Gannat), and University of Poitiers (La Milloque, Thézels, Paulhiac).

We used a multi-proxy approach to investigate palaeoecology, combining stable carbon and oxygen isotopes, dental mesowear and microwear, enamel hypoplasia and body mass estimation. The number of teeth studied for each method is detailed in table 1 by locality and species. Each method is detailed thereafter.

2.1. Body mass estimations

The body mass of mammals is linked to a large number of physiological and ecological traits [19,20], including metabolism rate, behaviour, habitat or spatial distribution. Although not the best proxies to estimate body mass, teeth were used here, as they are abundant and more often well-preserved in the fossil record than long bones [21,22]. Classical equations linking length and width of first and second upper and lower molars were used, as detailed in table 2. For each equation, we obtained the mean body mass of each species at each locality (if several teeth were available for one individual, only one by locus was randomly selected for the mean calculation at the locality). We then used the median of the means of all proxies to report for each species and locality.

2.2. Enamel hypoplasia

Tooth enamel develops early in life and is not remodelled afterwards. Teeth may record stresses that result in developmental hiatuses and growth defects. Among these defects, enamel hypoplasia is one

Table 1. List of rhinocerotid species found at each locality studied along with the number of specimens included for each method. Time ordering according to the following references [16–18].

			BM	microwear		mesowear	hypoplasia	stable isotopy
				Gr	Sh			
Gaimersheim	MP28	*Mesaceratherium gaimersheimense*	9	5	2	4	52	2
		Ronzotherium romani	16	4	4	2	91	7
Rickenbach	MP29*	*Brachydiceratherium lamilloquense*	8	2	1	3	14	0
		Mesaceratherium paulhiacense	4	3	2	2	13	7
		Ronzotherium romani	6	8	3	3	22	0
La Milloque	MP29	*Brachydiceratherium lamilloquense*	10	7	4	5	84	5
		Mesaceratherium paulhiacense	11	4	1	6	38	3
Thézels	MP30	*Brachydiceratherium* aff. *lemanense*	3	1	1	0	17	0
		Mesaceratherium gaimersheimense	34	12	12	8	154	5
Gannat	MP30 to MN1	*Brachydiceratherium lemanense*	22	16	12	5	132	13
		Pleuroceros pleuroceros	7	0	0	1	33	0
Tomerdingen	MN1	*Diaceratherium tomerdigense*	7	0	0	1	36	0
Paulhiac	MN1*	*Brachydiceratherium aginense*	2	1	0	3	12	0
		Brachydiceratherium lemanense	9	6	2	2	80	0
		Mesaceratherium paulhiacense	0	0	1	0	17	0
		Pleuroceros pleuroceros	2	0	1	0	8	0
Wischberg	MN1	*Brachydiceratherium lemanense*	3	2	0	0	6	0
		Pleuroceros pleuroceros	4	0	0	1	19	0
Pappenheim	MN2	*Brachydiceratherium lemanense*	3	3	0	1	12	0
Ulm-Westtangente	MN2a	*Mesaceratherium* cf. *paulhiacense*	27	11	5	12	149	5
		Protaceratherium minutum	64	21	9	16	317	3
Engehalde	MN2	*Brachydiceratherium aginense*	4	1	0	0	14	0
		Brachydiceratherium lemanense	5	0	0	1	23	0
Laugnac	MN2*	*Brachydiceratherium aginense*	18	3	0	3	100	0

(*Continued.*)

Table 1. (*Continued.*)

			BM	microwear		mesowear	hypoplasia	stable isotopy
Valquemado	MN2	*Protaceratherium minutum*	8	5	2	1	47	4
Loranca del Campo	MN3a	*Brachydiceratherium* cf. *aurelianense*	0	0	1	0	16	0
		Protaceratherium minutum	36	13	6	13	173	10
Wintershof-West	MN3	*Brachydiceratherium aurelianense*	4	3	2	1	14	0
		Mesaceratherium paulhiacense	3	4	0	1	10	0
		Protaceratherium minutum	1	1	0	0	1	0

*indicates that the locality is the reference of the Mammal Paleogene (MP) or Neogene (MN) zone.
BM, body mass; Gr, grinding facet; Sh, shearing facet.

Table 2. List of the dental proxies and the associated equations used in this study to estimate rhinocerotids' body mass. Measurements are in mm for all equations and give body mass in kg for Janis [23] and in g otherwise.

locus	equation	reference
m1		
	$\ln(m) = 1.5133 \times \ln(\text{m1 length x width}) + 3.6515$	[24]
	$\log(m) = 3.26 \times \log(\text{m1 length}/10) + 1.337$	[23]
m2		
	$\log(m) = 3.2 \times \log(\text{m2 length}/10) + 1.13$	[23]
	$\log(m) = 3.07 \times \log(\text{m2 length}) + 1.07$	[25]
M1		
	$\ln(m) = 3.19 \times \ln(\text{M1 length}) + 2.1$	[26]
M2		
	$\log(m) = 3.18 \times \log(\text{M2 length}/10) + 1.091$	[23]
	$\log(m) = 3.03 \times \log(\text{M2 length}) + 1.06$	[25]
	$\ln(m) = 3.09 \times \ln(\text{M2 length}) + 2.14$	[26]

of the most common [27]. Enamel hypoplasias are permanent and sensitive defects, but they are individual-dependant and non-specific. They have been linked to many causes including birth [28,29], weaning [30,31], diseases [32] or nutritional stress [29,30]. There is consensus on neither the method to study hypoplasia, nor on the threshold between normal and pathological enamel exists, so we chose to investigate hypoplasia with the naked eye, as it is faster, cheaper, more used, and less prone to false positives than microscopy approaches [33]. This method consists of the macroscopical spotting and identification of the defects according to the Fédération Dentaire Internationale categories (linear, pit and aplasia) and the caliper measurements of parameters (e.g. distance to enamel–dentine junction, width of the defect) related to timing, severity and duration of the defect. Other information recorded includes the number of defects, localization on the crown and degree of severity (figure 2).

2.3. Carbon- and oxygen-stable isotopes of the carbonates in the rhinocerotids' enamel

Carbon isotopic composition of teeth and bones is linked to the feeding behaviour (C3 or C4 plant preferences) and tracks habitat openness [35,36], while oxygen isotopic composition might inform on

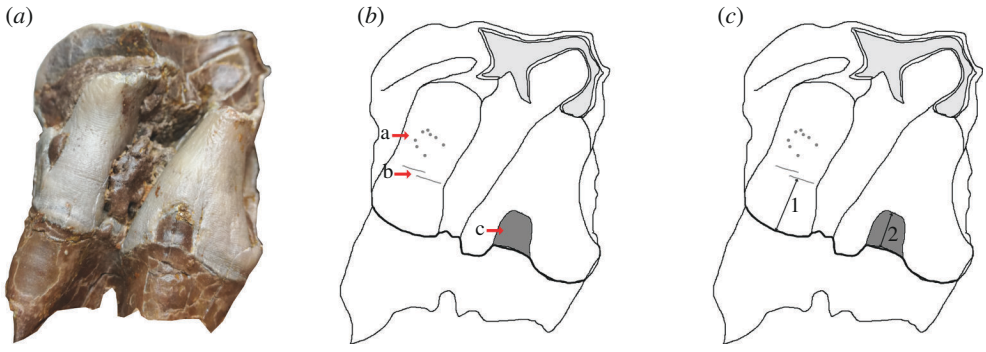

Figure 2. The three different types of hypoplasia defects considered in this study and the associated measurements. (*a*) Lingual view of right M2 of the specimen MHNT.PAL.2004.0.58 (*Hispanotherium beonense*) displaying three types of hypoplasia defects. (*b*) Interpretative drawing of the photo in (*a*) illustrating the hypoplastic defects: a, pitted hypoplasia; b, linear enamel hypoplasia; and c, aplasia. (*c*) Interpretative drawing of the photo in (*a*) illustrating the measurements: 1, distance between the base of the defect and the enamel-dentin junction; 2, width of the defect (when applicable). Figure from Hullot *et al*. [34].

the temperature and precipitation [36,37]. Here, we have focused on the signal from the carbonates of tooth enamel from rhinocerotids, as both isotopes can be studied at the same time (faster and cheaper).

Not all localities were sampled for isotopic analyses, due to sampling restrictions (destructive and costly), but we provided a coverage of all biostratigraphic zones of the MP28 to MN3 interval. Rhinocerotid teeth from the following localities were sampled: Gaimersheim (MP28), La Milloque (MP29), Thézels (MP30), Gannat (MP30-MN1), Ulm-Westtangente (MN2), Valquemado (MN2) and Loranca del Campo (MN3). Additionally, we included data from the literature for the locality of Rickenbach (MP29) [38]. Some specimens from La Milloque, Thézels and Gannat were also serially sampled to investigate seasonality close to the Oligocene–Miocene boundary and the Mi−1 event.

Sampling was done on a restricted zone close to the root−crown junction (last part of the crown to develop, punctual) or along the crown (serial) on identified isolated teeth or fragments, preferably from third molars to avoid pre-weaning or weaning signal. After mechanical cleaning with a Dremel® equipped with a diamond tip, enamel powder was sampled. As we focused on carbonates, carbon and oxygen isotopic composition could be studied at the same time, limiting the amount necessary for the analyses (between 500 and 1000 µg). Organic matter was removed following standard procedures [39] and the samples were then acidified with phosphoric acid (103%), producing CO_2 analysed for isotopic content using a ThermoFisher Kiel IV carbonate device connected to a Thermo Scientific Delta V+ stable isotope ratio mass spectrometer (AETE-ISO platform, OSU-OREME, University of Montpellier). The within-run precision (± 1 σ) of these analyses as determined by the replicate analyses of NBS 18 and AIEA-603 was less than ± 0.2‰ for $\delta^{13}C$ and ± 0.3‰ for $\delta^{18}O$ ($n = 5, 6$, respectively). Results are expressed as ratio (‰) to the Vienna-Pee Dee Belemnite (VPDB) standard as follows:

$$\delta = 1000 \times \left(\frac{R_{sample}}{R_{standard}} - 1 \right)$$ where R_{sample} refers to the ratio of $\frac{^{13}C}{^{12}C}$ and $\frac{^{18}O}{^{16}O}$ of the sample and $R_{standard}$ to the VPDB.

The $\delta^{13}C_{diet}$ can be obtained from $\delta^{13}C_{CO3,\ enamel}$ taking into account the body mass and the digestive system as detailed below [40]

$$\varepsilon^*_{diet-bioapatite} = e^{2.42 + 0.032 \times ln(bodymass)}$$

$$\delta^{13}C_{diet} = \delta^{13}C_{CO3,\ enamel} - \varepsilon^*_{diet-bioapatite} - corr$$ where corr is the correction factor for the variation of $\delta^{13}C_{CO2}$ of the atmosphere. Post-1930, the values of $\delta^{13}C_{CO2}$ are −8‰ [7]. Depending on the locality, the reconstructed values based on benthic foraminifera [41] are higher than today with estimates between −6.1 and −5.7‰. The $\delta^{13}C_{diet}$ is then used to infer the mean annual precipitations (MAP) with the equation from Kohn [42]: $MAP = 10\left(\frac{-\delta^{13}C_{diet} + 10.29 + 0.0124 \times |latitude| - 1.9 \times 10^{-4} \times altitude}{5.61}\right) - 300$ or that of Rey *et al*. [43]: $MAP = 10^{0.092 \times \Delta^{13}C_{leaf} + 1.148} - 300$ where $\Delta^{13}C_{leaf} = \frac{\delta^{13}C_{atm} - \delta^{13}C_{diet}}{1 + \frac{\delta^{13}C_{diet}}{1000}}$.

Regarding oxygen, the $\delta^{18}O_{CO3(V\text{-}PDB)}$ was converted into $\delta^{18}O_{CO3(V\text{-}SMOW)}$ using the equation from Coplen *et al*. [44]: $\delta^{18}O_{V-SMOW} = 1.03091 \times \delta^{18}O_{V-PDB} + 30.91$. This was used to calculate the $\delta^{18}O_{precipitation}$

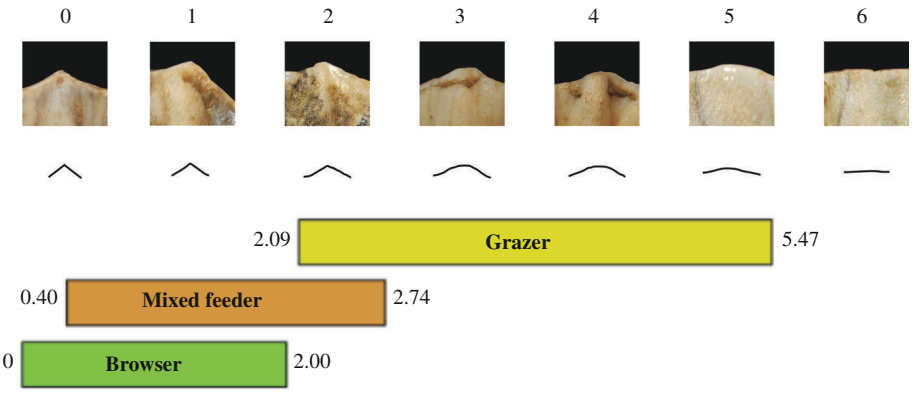

Figure 3. Mesowear score with the mesowear ruler method illustrated with rhinoceros' (*Coelodonta antiquitatis*) cusps and interpretative drawings. Modified from Jiménez-Manchón *et al*. [53].

and the mean annual temperature (MAT) detailed as follows. No reliable equation to estimate the $\delta^{18}O_{precipitation}$ based on the $\delta^{18}O_{enamel}$ of rhinoceros is available in the literature, so we used an equation designed for elephants [45], as their metabolism (hindgut fermenter) and size (megaherbivore) are close to that of rhinoceros [15]. The $\delta^{18}O$ in the following equations are expressed in relation to the Vienna Standard Mean Ocean Water (V-SMOW): $\delta^{18}O_{PO4} = 0.94 \times \delta^{18}O_{precipitation} + 23.3$ equation from Ayliffe *et al*. [45] for modern elephants and $\delta^{18}O_{PO4} = 0.96 \times \delta^{18}O_{CO3} - 8.05$ relation phosphates-carbonates from Lécuyer *et al*. [46].

Hence $\delta^{18}O_{precipitation} = 1.02 \times \delta^{18}O_{CO3} - 33.3$

Eventually, the MAT can be calculated using the obtained $\delta^{18}O_{precipitation}$,

$$MAT = \frac{\delta^{18}O_{precipitation} + 14.178}{0.442}$$ [47] or $MAT = 1.41 \times \delta^{18}O_{precipitation} + 23.63$ [48].

2.4. Dental wear: mesowear ruler and dental microwear texture analyses

To provide more robust dietary inferences, we combined mesowear and microwear. Both proxies give insights at different time scales: days to weeks for microwear and long-term cumulative over life for mesowear [49,50]. Mesowear is the categorization of macroscopical dental wear of labial cusp shape (relief and sharpness) into scores that can be used to infer individual dietary preferences within the classical herbivore diet categories: browser, mixed-feeder and grazer [51]. Here, we used the mesowear ruler [52], which gives scores ranging from 0 (cusp high and sharp) to 6 (cusp low and blunt; figure 3). We only scored the paracone of upper molars (mostly M1–2, but two M3 were included) with an average wear (wear stages 4 to 7 from Hillman-Smith *et al*. [54], and not the sharpest cusp (metacone or paracone), as significant differences have been noted between these two cusps in rhinoceros [34,55]. With this approach, browsers have low scores (mean of extant species reported in the literature between 0 and 2) and grazers high ones (2.09–5.47), while mixed-feeders have intermediate values (0.4–2.74) [53]. Despite the wide use of the mean for mesowear data in the literature [50,52,56,57], we chose to use the median in this study. Indeed, the mesowear ruler yields ordinal categorical scores, which implies that the mean would assume equidistant categories or would not make sense mathematically.

Dental microwear texture analyses (DMTA) investigate tooth surfaces and identify wear patterns associated with the different diet categories. We followed a protocol adapted from Scott *et al*. [58] using scale-sensitive fractal analyses and completed the overview with ISO parameters [59]. Facets representing both phases of the mastication (grinding and shearing) were sampled on the same enamel band near the protocone, protoconid or hypoconid (figure 4). After thorough cleaning with acetone, we moulded twice well-preserved wear facets of molars (upper and lower, left and right) using dentistry silicone (Coltene Whaledent PRESIDENT The Original Regular Body ref. 60019939). The second mould was used for the analyses described hereafter.

The moulded facet was put flat under the 100× objective (Leica Microsystems; Numerical aperture: 0.90; working distance: 0.9 mm) of the Leica Map DCM8 profilometer hosted at the PALEVOPRIM Poitiers (TRIDENT), and scanned using white light confocal technology. Using LeicaMap (v. 8.2; Leica Microsystems), we pre-treated the obtained scans (.plu files) as follows: inversion of the surface (as they are negative replicas of the actual surface), replacement of the non-measured points (less than

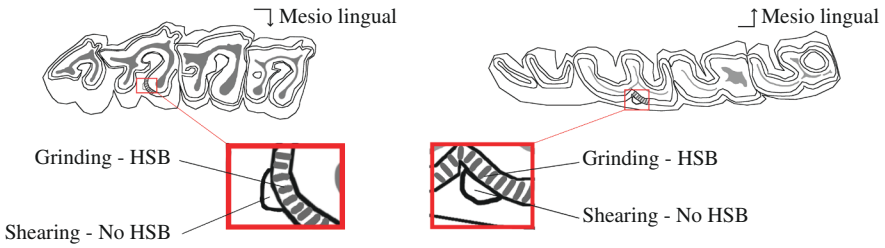

Figure 4. Localization of the microwear facets on rhinocerotid molars. Position of the two microwear facets (grinding and shearing) near the protocone on the second upper molar (left) and near the protoconid on second lower molar (right). Both facets are sampled on the same enamel band with (grinding) or without (shearing) Hunter-Schreger bands (HSB). Modified after Hullot *et al*. [60].

1%) by the mean of the neighbouring points, removal of aberrant peaks [61], levelling of the surface, removal of form (polynomial of degree 8) and selection of a 200 × 200 µm area (1551 × 1551 pixels) saved as a digital elevation model (.sur) to be further analysed. Textural and ISO parameters of the selected surfaces (200 × 200 µm) were then estimated in MountainsMaps® (v. 8.2). Our study will focus on the following texture variables, described in detail in Scott *et al*. [62]:

- anisotropy measures the orientation concentration of surface roughness. Several parameters can indicate the anisotropy of the surface:
  - (i) epLsar (exact proportion of length-scale anisotropy of relief) or NewepLsar. The latter is the corrected value of epLsar in MountainsMaps® compared with Toothfrax (software previously used for DMTA but not supported anymore) as there was an error in the code to calculate this parameter in Toothfrax [63];
  - (ii) Str is a spatial parameter of the international standard ISO 25178 (specification and measurement of three-dimensional surface textures). It is the ratio of Rmin/Rmax, where Rmin and Rmax are, respectively, the minor and major axes of the intersection ellipse between the plane z = s with the autocorrelation function $f_{ACF}(tx, ty)$. Rmin is the autocorrelation length, i.e. the horizontal distance of the $f_{ACF}(tx, ty)$, which decays fastest to a specified value s between 0 and 1. Here, we considered s = 0.5. Low values of Str indicate strong anisotropy;
- complexity or area-scale fractal complexity (Asfc) evaluates the roughness at a given scale;
- heterogeneity of the complexity (Hasfc) investigates the variation of complexity at a given scale (here 3 × 3 and 9 × 9) within the studied 200 × 200 µm area.

The interpretation of DMTA signatures in fossil specimens is based here on the values and thresholds proposed in extant species [60,64]. Moreover, we used a dataset of extant species of rhinoceroses and tapirs with their associated inferred diets [60,65]. The dataset consists of 17 specimens of *Ceratotherium simum*, four of *Dicerorhinus sumatrensis*, 21 of *Diceros bicornis*, 15 of *Rhinoceros sondaicus* (one new specimen), five of *Rhinoceros unicornis* (one new specimen) and 15 of *Tapirus terrestris*. Results of DMTA for these species are available in electronic supplementary material, S2, figure 1.

2.5. Statistics and figures

Statistics and figures were done in R (v. 4.2.3) equipped with ggplot2 [66], cowplot [67] and gridExtra [68]. Inkscape (v. 1.0.1) was also used for figures. We favoured the use of non-parametric tests, due to limited sample size at some localities, which prevents from testing if the distribution of the data is normal (table 1). For microwear data, however, we used a Box-Cox transformation to apply the parametric MANOVA and ANOVA. Following the recent statement of the American Statistical Association (ASA) on *p*-values [69], we favoured giving exact values and we tried to be critical regarding the classical thresholds of 'statistical significativity'.

Table 3. Summary of the results for body mass, enamel hypoplasia, stable isotopy (carbon and oxygen) and mesowear for the rhinocerotids of the Oligocene–Miocene transition. Mean (median for mesowear as it is categorical) by locality and by species for each parameter.

	body mass (kg)	hypoplasia (%)	$\delta^{13}C_{CO3,\ enamel}$ (‰ V-PDB)	$\delta^{18}O_{CO3,\ enamel}$ (‰ V-PDB)	mesowear
Gaimersheim (MP28)					
Mesaceratherium gaimersheimense	800	5.77	−10.5	−5.6	2
Ronzotherium romani	2370	13.19	−10.3	−6.1	1.5
Rickenbach (MP29)					
Brachydiceratherium lamilloquense	1600	42.86	−10	−4.4	2
Mesaceratherium gaimersheimense	1240	46.15	—	—	2
Ronzotherium romani	1820	4.55	−10.9	−8.9	4
La Milloque (MP29)					
Brachydiceratherium lamilloquense	1290	20.24	−10.5	−3.8	1
Mesaceratherium paulhiacense	940	10.53	−10.3	−3.5	2
Thézels (MP30)					
Brachydiceratherium aff. *lemanense*	1650	0	—	—	—
Mesaceratherium gaimersheimense	850	7.14	−8.8	−3.4	2
Gannat (MP30-MN1)					
Brachydiceratherium lemanense	1760	21.21	−8.1	−3.4	2
Pleuroceros pleuroceros	740	6.06	—	—	2
Tomerdingen (MN1)					
Diaceratherium tomerdingense	1440	16.67	—	—	4
Paulhiac (MN1)					
Brachydiceratherium aginense	2000	16.67	—	—	1
Brachydiceratherium lemanense	1210	1.25	—	—	2.5
Mesaceratherium paulhiacense	820	11.76	—	—	—
Pleuroceros pleuroceros	680	25	—	—	—
Wischberg (MN1)					
Brachydiceratherium lemanense	1450	66.67	—	—	—
Pleuroceros pleuroceros	660	0	—	—	2
Pappenheim (MN2)					
Brachydiceratherium lemanense	2000	50	—	—	2
Ulm-Westtangente (MN2a)					
Mesaceratherium cf. *paulhiacense*	1880	17.45	−10.6	−5.3	2.5
Protaceratherium minutum	500	16.72	−8.1	−5.1	2
Engehalde (MN2)					
Brachydiceratherium aginense	1060	28.57	—	—	—
Brachydiceratherium lemanense	1160	17.39	—	—	2
Laugnac (MN2)					
Brachydiceratherium aginense	1770	14	—	—	2
Valquemado (MN2)					
Protaceratherium minutum	670	8.51	-9	−3.1	0
Loranca (MN3a)					

(*Continued.*)

Table 3. (*Continued.*)

	body mass (kg)	hypoplasia (%)	$\delta^{13}C_{CO3}$, enamel (‰ V-PDB)	$\delta^{18}O_{CO3}$, enamel (‰ V-PDB)	mesowear
Brachydiceratherium cf. *aurelianense*	—	18.75	—	—	—
Protaceratherium minutum	660	14.45	−9.1	−3.1	2
Wintershof-West (MN3)					
Brachydiceratherium aurelianense	1370	28.57	—	—	3
Mesaceratherium paulhiacense	1000	10	—	—	1
Protaceratherium minutum	580	0	—	—	—

3. Results

3.1. Body mass estimations

The sample studied includes six genera of rhinocerotids. All the species of three genera—*Ronzotherium*, *Brachydiceratherium* and *Diaceratherium*—were large-sized rhinoceros, exceeding the megaherbivore threshold of 1000 kg [15]. For *R. romani*, the mean body mass was estimated between 1800 and 2400 kg (table 3). Regarding the two teleoceratines, the mean body mass estimates of *Brachydiceratherium* spp. range from 1000 to 2000 kg depending on the locality and the species, whereas *D. tomerdigense* (monotypic genus, found only in Tomerdingen) reached about 1500 kg (table 3).

Mesaceratherium species were slightly smaller, with an average body mass ranging from 800 to 1300 kg, except at Ulm-Westtangente were *M. paulhiacense* mean body mass reached 1900 kg. However, a revision of the rhinocerotid material is needed at this locality and a third species could be present (*Plesiaceratherium platyodon*). Eventually, the last two species were small-sized rhinoceros: *Pleuroceros pleuroceros* mean body mass was approximately 650–750 kg, slightly bigger than *Protaceratherium minutum* with mean body mass between 500 and 700 kg depending on localities.

3.2. Hypoplasia prevalence

In total, 251 teeth out of the 1704 (14.73%) examined for hypoplasia showed at least one defect, representing a rather moderate global prevalence of hypoplasia during the Late Oligocene–Early Miocene interval. There were, however, clear differences between species, localities and time intervals (table 3; figure 5). Rhinocerotids from Oligocene localities had a lower global prevalence of hypoplasia (12.37%; 60/485 teeth) than the Miocene ones (15.28%; 161/1054), but the difference was not statistically significant (Pearson's Chi-squared test X-squared = 4.0618, d.f. = 2, p-value = 0.1312; electronic supplementary material, S1). When considering the biostratigraphical units (MP and MN zones), some pairs had low p-values (between 0.0594 and 0.005) when compared with a pairwise Wilcoxon test (electronic supplementary material, S1). This revealed time intervals of low hypoplasia prevalence (less than 11%) during MP28, MP30 and MN1, and intervals of higher prevalence (between 15 and 20%) during MP29, MN2 and MN3. The different zones contained, however, various numbers of specimens and localities (only one locality: MP28, Gaimersheim; MP30, Thézels; MN2 dominated by Ulm-Westtangente).

Concerning genus, *Brachydiceratherium* was the most affected with about 17.75% (93/524) of studied teeth having hypoplasias. *Brachydiceratherium* was also the most common genus, present at nearly all localities. In contrast, *Pleuroceros* had the lowest frequency of hypoplasia (4/60 = 6.67%), but this genus was only found at two localities (Gannat and Wischberg) and totalling 60 teeth. Eventually, the other genera (*Diaceratherium*, *Ronzotherium*, *Mesaceratherium* and *Protaceratherium*) had similar hypoplasia prevalence (pairwise Wilcoxon, p-values > 0.22; electronic supplementary material, S1), oscillating between 12 and 17% of hypoplastic teeth.

Regarding locality, the prevalence of hypoplasia was moderate (greater than 10%) to high (greater than 20%) at all of them, except at Valquemado (4/47, 8.51%), Thézels (11/171, 6.43%) and Paulhiac (7/117, 5.98%) where it was low. The rhinocerotids from Pappenheim (6/12 teeth, 50%), Rickenbach

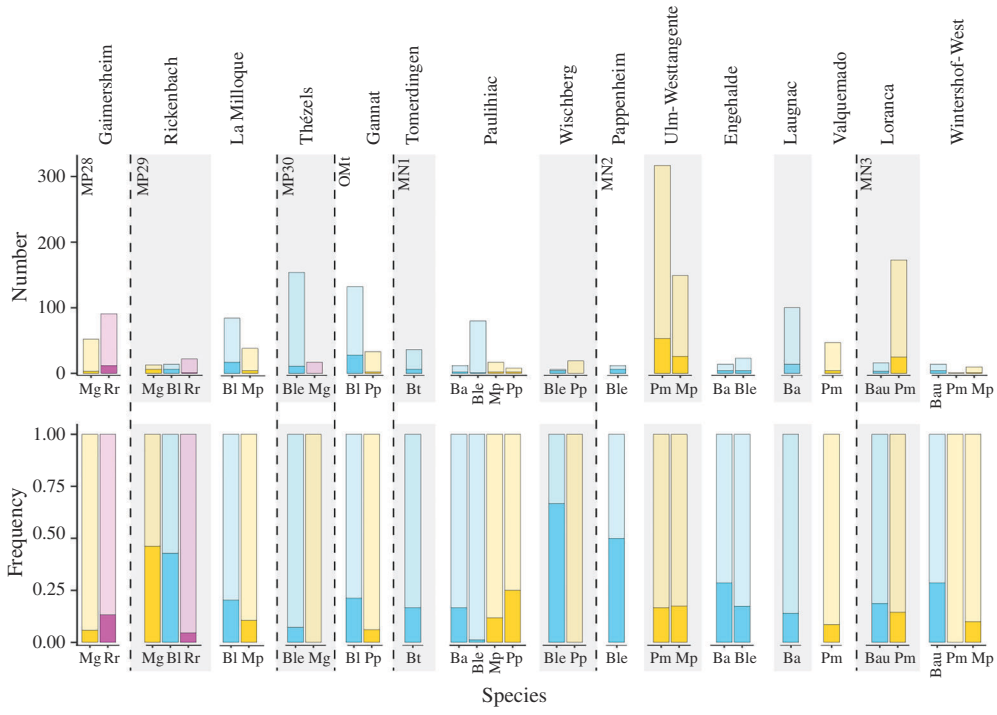

Figure 5. Hypoplasia prevalence by rhinocerotid species and locality of the Oligocene–Miocene transition. Abbreviations: Ba, *Brachydiceratherium aginense*; Bau, *B. aurelianense*; Bl, *B. lamilloquense*; Ble, *B. lemanense*; Dt, *Diaceratherium tomerdingense*; Mg, *Mesaceratherium gaimersheimense*; Mp, *M. paulhiacense*; Pm, *Protaceratherium minutum*; Pp, *Pleuroceros pleuroceros*; Rr, *Ronzotherium romani*. Colour code: blue, Teleoceratiina; yellow, aceratheres *sensu* lato; pink, basal stem rhinocerotids. Dark shades indicate hypoplastic teeth, while light shades show unaffected ones.

(13/49, 26.53%) and Engehalde (8/37, 21.62%) were the most affected, but the sample sizes were much smaller. A pairwise Wilcoxon test confirmed differences between most pairs of least affected versus most affected localities (p-values < 0.05; electronic supplementary material, S1).

3.3. Enamel stable isotopy (carbon and oxygen)

All specimens were in the range of C3 feeding, with values of the $\delta^{13}C_{diet}$ comprising between −27.9 and −23.1‰. There was a clear shift towards higher values of $\delta^{13}C_{diet}$ for rhinocerotoids between La Milloque (MP29) and Thézels (MP30; figure 6). The cut-off for this shift is around −25.6‰, very close to the modern biotopes threshold between woodland-mesic C3 grassland and open woodland-xeric C3 grassland (−25‰; figure 6). All specimens from Gaimersheim, Rickenbach and La Milloque had values of $\delta^{13}C_{diet}$ below this biotopes threshold, whereas most specimens of Loranca and Thézels had values close to −25‰ or slightly above (± 0.5‰). The specimens from Valquemado (*P. minutum*, n = 4), Gannat (*B. lemanense*, n = 13) and Ulm-Westtangente were on both sides of the threshold (low values for *M. paulhiacense*, n = 4; high values for *P. minutum*, n = 3). The lowest values of $\delta^{13}C_{diet}$ are mostly specimens of *B. lamilloquense* and *M. paulhiacense*, whereas the highest values are specimens of *P. minutum* and *B. lemanense*.

Regarding the oxygen content, values of the $\delta^{18}O_{CO3,\ SMOW}$ ranged from 24 to 29.2‰. All specimens from Gaimersheim (*R. romani*, n = 6; *M. gaimersheimense*, n = 2), clustered together and displayed the lowest range of values ($\delta^{18}O_{CO3,\ SMOW} \leq 25.1$‰), whereas the ones from La Milloque (*B. lamilloquense*, n = 6; *M. paulhiacense* n = 3) took a wide range of values from 25.5 to 27.8‰. Similarly to the $\delta^{13}C_{diet}$, there is a chronological shift in the values of $\delta^{18}O_{CO3,\ SMOW}$ between La Milloque and Thézels. The values at Ulm-Westtangente (MN2) are, however, more similar to the Oligocene ones.

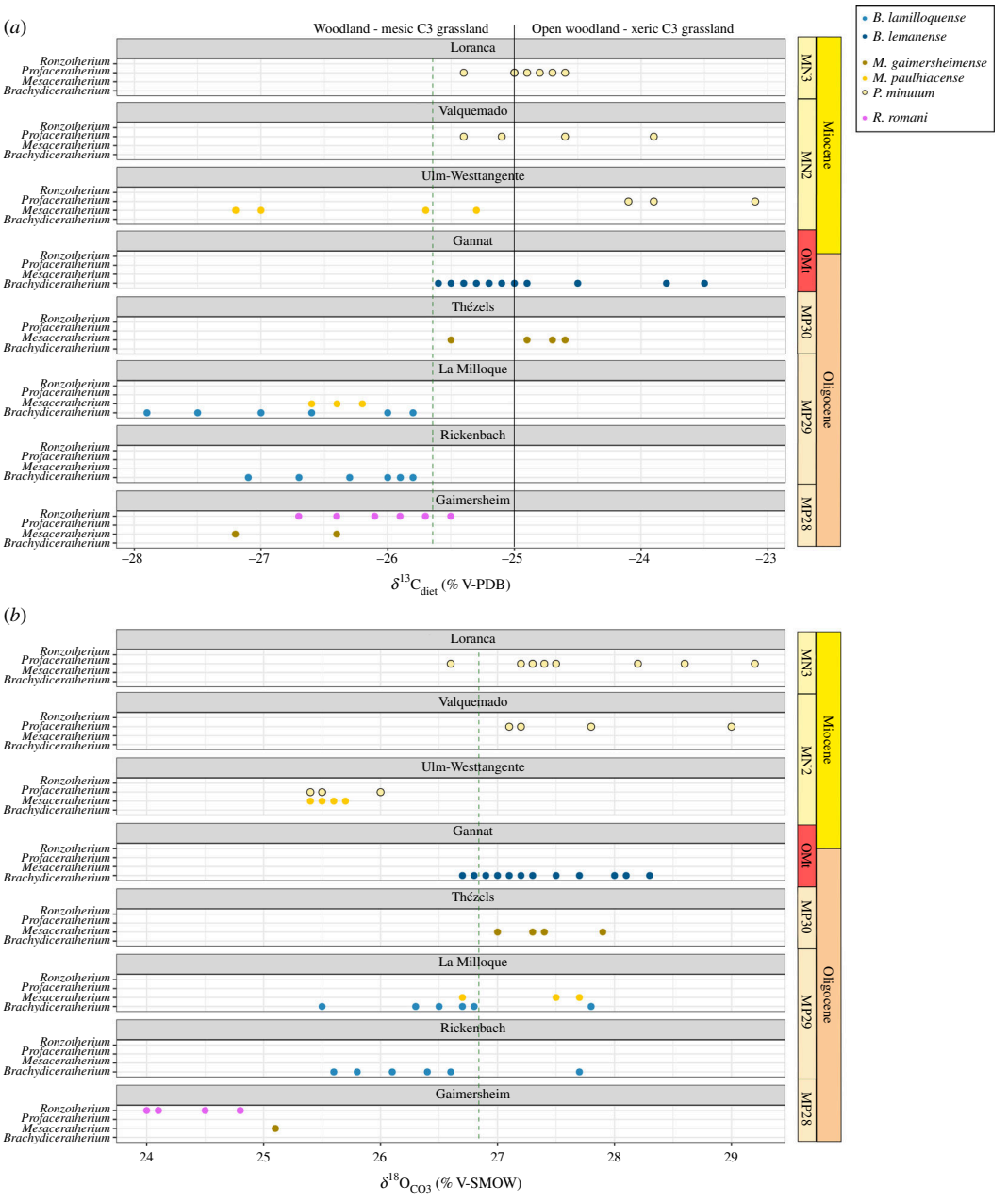

Figure 6. Carbon (*a*) and oxygen (*b*) content of the diet and enamel of rhinocerotids from various late Oligocene to early Miocene localities. Green dashed lines: shift, black lines: cut-offs between different biomes. Colour code by species as detailed in the figure.

3.4. Dental wear: mesowear and microwear

Depending on the locality and the species, the median mesowear score was between 0 (*P. minutum* at Valquemado, $n = 1$) and 4 (*D. tomerdingense* at Tomerdingen, $n = 1$ and *R. romani* at Rickenbach, $n = 3$). About half of the median values by species and localities (13/24, table 3) were, however, equal to 2, suggesting browsing or mixed feeding habits. The sample size of each species at each locality was often small ($n < 5$) or null due to preservation issues (table 1), which limited the statistical power to compare localities and species' spatio-temporal evolution.

Wilcoxon test revealed differences in mesowear scores at the species and genus levels. Pairwise tests failed to detect clear differences between species (p-values > 0.18), but highlighted some at the genus level (probably due to greater sample size), between *Mesaceratherium* and *Brachydiceratherium* (p-value = 0.021), and between *Mesaceratherium* and *Protaceratherium* (p-value = 0.057). Indeed, *Mesaceratherium* had greater mesowear scores than both other genera, suggesting more abrasive dietary preferences for *Mesaceratherium* specimens. There were, however, little changes by species between the different time

intervals and localities (table 3, electronic supplementary material, S1), indicating limited evidence for dietary changes over space and time within our sample.

The DMTA revealed more differences, although most of the sampled fossil rhinocerotids fell in the range of extant browsers or mixed-feeders. We conducted a MANOVA on DMTA variables (Asfc, NewepLsar, H9, H81 and Str) by facet, species and locality (parameters). All parameters had a marked influence (p-values < 10^{-4}) on the DMT signature observed. To obtain precise differences, we ran an ANOVA for each variable. Both H9 and H81 had no difference for any parameters nor interaction of parameters (e.g. species ∗ locality). Regarding Asfc, all parameters showed differences (p-values < 0.02). In the case of NewepLsar only facet had a marked influence (p-value = 0.00132). Eventually, for Str, species (p-value = 3.67×10^{-16}), locality (p-value = 1.09×10^{-8}) and the interaction of species with locality (p-value = 0.051) all had a marked influence. As locality and species had more than two states, we used least significant difference (LSD) post hoc tests to investigate the differences highlighted by the ANOVAs for Asfc and Str.

The LSD post hocs (electronic supplementary material, S1) did not reveal specific pairs with differences regarding Asfc for locality and only one for species (*P. minutum* and *B. lemanense*; p-value = 0.0111). Concerning Str, several pairs had low p-values for both locality and species. Most species differences were attributed to *M. gaimersheimense*, that had lower Str values than all other species studied (p-values < 0.0393), except *B. aurelianense*. Some differences were also observed for *B. lamilloquense* (high Str values) compared with *P. minutum* (p-value = 7.89×10^{-6}), *B. lemanense* (p-value = 0.0278) and *M. paulhiacense* (0.0713) and for *P. minutum* (low Str values) compared with *B. aginense* (p-value = 0.0084; electronic supplementary material, S1). Similarly, all differences for locality were found in pairs containing either Rickenbach (higher Str values) and/or Thézels (lower Str values).

As Asfc and Str were the two parameters with the most variations for species and locality, we plotted them (figure 7). Contrary to mesowear, DMT signature changed over time and space for some species (see also electronic supplementary material, S2, figure 2 for a plot by species). Major changes of dietary preferences were observed for *B. lemanense*, which shows a decrease of anisotropy (inverse of Str) and increase of complexity (Asfc) between the MP30 (Thézels, grinding: mean Str = 0.12, mean Asfc = 1.23) and the MN2 (Pappenheim, grinding: mean Str = 0.73, mean Asfc = 2.01), except at Wischberg (grinding: mean Str = 0.34, mean Asfc = 1.14). Important variations of DMT are also found for *M. gaimersheimense*, which oscillates from a mixed-feeder profile at Gaimersheim, browser at Rickenbach (grinding: mean Str = 0.80, mean Asfc = 2.31) and to a very abrasive diet at Thézels (grinding: mean Str = 0.14, mean Asfc = 1.18). More subtle variations were found for *M. paulhiacense* with a more complex and anisotrope texture at Wintershof-West (grinding: mean Str = 0.41, mean Asfc = 2.29) than at La Milloque (grinding: mean Str = 0.57, mean Asfc = 1.90) and Ulm-Westtangente (grinding: mean Str = 0.56, mean Asfc = 1.32), for which the signatures are relatively similar. Eventually, *P. minutum* have slightly higher complexity and lower anisotropy at the Iberian localities (Valquemado, grinding: mean Str = 0.51, mean Asfc = 2.21; Loranca del Campo, grinding: mean Str = 0.45, mean Asfc = 1.98) than at Ulm-Westtangente.

3.5. General results and evolutionary trends

Body mass, mesowear and hypoplasia prevalence were tracked by species and locality and plotted alongside (figure 8, mesowear in electronic supplementary material, S2, figure 3). Similar trends were observed for all parameters, notably body mass and hypoplasia (rho = 0.3365995, S = 2982, p-value = 0.06895), but depended on species. Teleoceratines and aceratheres *sensu lato* were the most common rhinocerotids in the dataset, found at nearly all localities and allowing temporal tracking of the variations. *Brachydiceratherium lamilloquense* is the oldest species of teleoceratines in the dataset, present only during MP29 at Rickenbach and La Milloque. Body mass (1600 → 1290 kg), prevalence of hypoplasia (42.85 → 20.24%) and median mesowear ruler (2 → 1) all decrease between Rickenbach and the slightly younger La Milloque (figure 8; electronic supplementary material, S2, figure 3). During the latest Oligocene and early Miocene (MP30–MN2), *B. lamilloquense* is replaced by *B. lemanense*. This second species is documented at many localities (Thézels, Gannat, Paulhiac, Wischberg, Pappenheim, Engehalde). The median mesowear ruler scores remain similar at 2 during the interval except at Paulhiac (2.5), but greater variation of body mass and hypoplasia prevalence are noted (figure 8). First, there is an increase during late Oligocene (Thézels: 1650 kg, 0% → Gannat: 1760 kg, 21.21%), then a decrease during the earliest Miocene (Paulhiac: 1210 kg, 1.25%), followed by a peak at Wischberg (1450 kg, 66.67%) and a final decrease during MN2 (Engehalde: 1160 kg, 17.39%). Another species was also found during the earliest Miocene (Aquitanian: MN1–MN2): *B. aginense*. For this species,

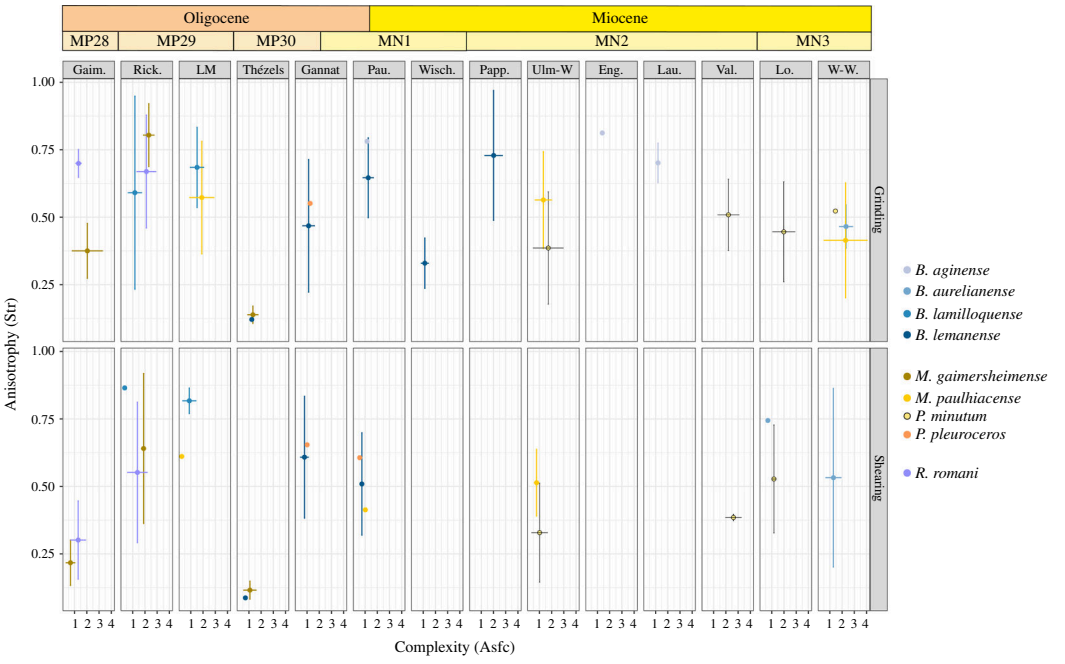

Figure 7. Anisotropy (Str) against complexity (Asfc) by locality and species. Localities ordered chronologically from the oldest (left) to the youngest (right): Gaimersheim (MP28), Rickenbach (MP29), La Milloque (MP29), Thézels (MP30), Gannat (MP30-MN1), Paulhiac (MN1), Wischberg (MN1), Pappenheim (MN2), Ulm-Westtangente (MN2a), Engehalde (MN2), Laugnac (MN2), Valquemado (MN2), Loranca del Campo (MN3a) and Wintershof-West (MN3). Colour code by species as detailed in the figure.

different trends are observed for the three parameters: body mass drops at Engehalde (1060 kg versus 2000 kg at Paulhiac [older] and 1770 kg at Laugnac [younger]) while hypoplasia prevalence peaks at this same locality (28.57% versus 16.67% at Paulhiac and 14% at Laugnac), and mesowear increases between Paulhiac and Laugnac (1 versus 2 respectively). Eventually, *B. aurelianense* is found during the MN3. Body mass (1370 kg) and mesowear ruler (3) were only available at Wintershof-West, while hypoplasia was recorded at both MN3 locality (18.75% at Loranca and 28.57% at Wintershof-West), but the sample size was limited (figure 8). *Diaceratherium tomerdigense*, another species of teleoceratines, was also studied here, but the species is only found in one locality (Tomerdingen, MN1).

Regarding, the aceratheres *sensu lato*, *Mesaceratherium gaimersheimense* is only recorded during Late Oligocene. This species exhibits stable mesowear median (2 at all localities) during the interval and similar trends for body mass and hypoplasia prevalence, with a peak at Rickenbach for the first two variables (1240 kg, 46.15%), while Gaimersheim and Thézels had similar values (about 800 kg, less than 10%). During Early Miocene, the aceratheres *sensu lato* included *M. paulhiacense* and *P. minutum*. The first one shows a peak in all parameters at Ulm-Westtangente (1880 kg, 17.45%, 2.5), and similar values of body mass and hypoplasia prevalence at the other localities (800–1000 kg, 10–12%; figure 8). *Protaceratherium minutum* has similar mean body mass estimates at all four localities where it was recorded (Ulm-Westtangente, Valquemado, Loranca del Campo and Wintershof-West), between 500 and 670 kg. Mesowear median and hypoplasia prevalence are similar for Ulm-Westtangente and Loranca del Campo (2, approx. 15%), but lower at Valquemado (8.51%, 0). Hypoplasia prevalence was null at Wintershof-West but very few specimens were available (figure 8).

Lastly, two species of basal rhinocerotidae were studied. *Pleuroceros pleuroceros* had similar mean body mass estimates (700 kg) and median mesowear ruler (2) at Gannat, Paulhiac (only mass) and Wischberg (figure 8; electronic supplementary material, S2, figure 3). Hypoplasia prevalence was low or null hypoplasia except at Paulhiac (25%), but the sample size for this species was very limited. *Ronzotherium romani* is a strictly Oligocene taxa. Body mass drastically diminished during the Late Oligocene (Gaimersheim: 2370 kg → Rickenbach: 1820 kg), similarly to hypoplasia prevalence (Gaimersheim: 13.19% → Rickenbach: 4.55%), but contrary to median mesowear that increased during this interval (Gaimersheim: 1.5 → Rickenbach: 4; figure 8; electronic supplementary material, S2, figure 3).

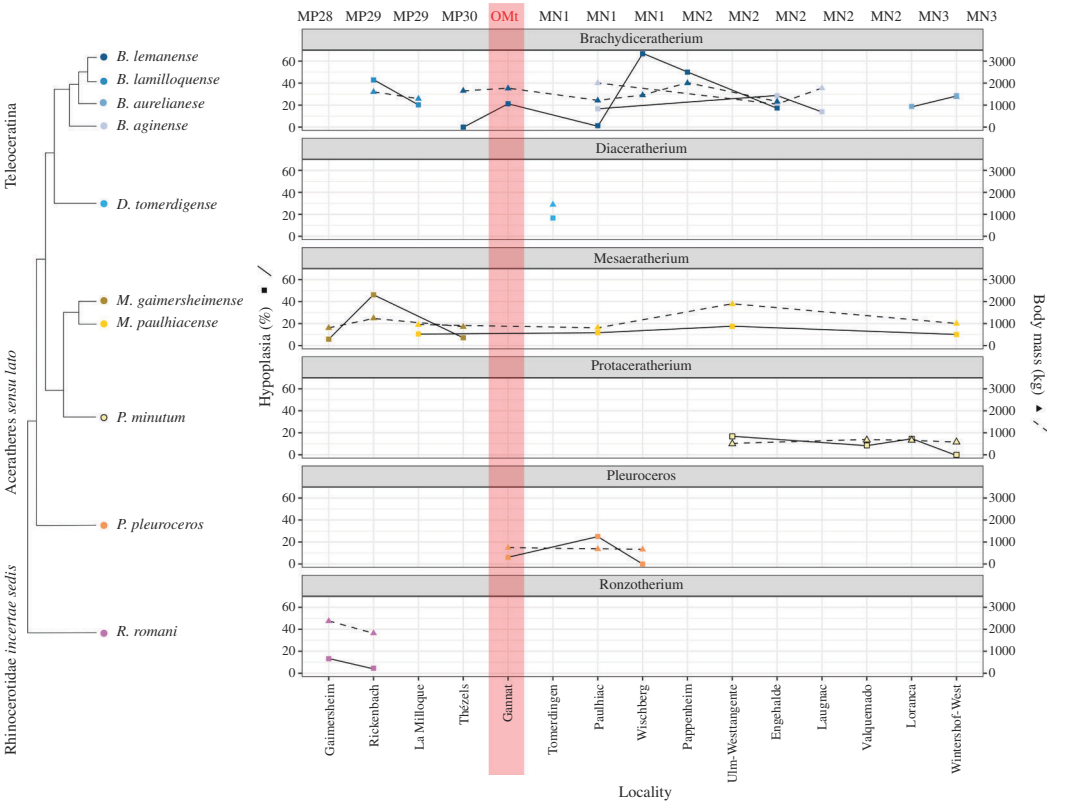

Figure 8. Hypoplasia prevalence (full line) and body mass (dashed line) by species and locality. Phylogenetic relationships based on the literature [70–73].

4. Discussion

4.1. Dietary preferences and niche partitioning of the rhinocerotids studied

All rhinocerotids studied fell within the range of C3 feeding for stable isotopes ($\delta^{13}C_{diet} < -22‰$) [74], and in the range of browsers (0–2) or mixed-feeders (0.4–2.74) for mesowear [53]. Although extant grazers have reported mean mesowear scores as low as 2.09 (*Kobus ellipsiprymnus*, *Redunca redunca*), a grazing diet seems unlikely for late Oligocene—early Miocene rhinocerotids in Europe. Indeed, even though C4 grasses were present locally in Southern Europe as soon as the early Oligocene [75], they were never dominant in Europe [76–78]. Regarding the second type of grasses, C3 grasslands were also limited in Europe at that time, as most of the continent was covered by forests and woodlands [78]. Moreover, C3 grasses contain lower levels of fibres, silica and toughness than their C4 counterparts [79], and hence C3 grazing should result in a lower abrasion load and mesowear scores.

Mesowear score is rather stable across time, space and taxa, with most species having a median mesowear score around 2 at the different localities. Similarly to other studies [80–82], we did not find a clear relationship between body mass and mesowear, suggesting once again that the classical assumption of greater tolerance for a lower-quality diet in larger species lacks empirical support [83].

At some localities, we highlighted some differences in the feeding preferences of the rhinocerotid specimens associated, which could indicate a potential niche partitioning (figure 9). On the contrary, potential competition for resources or different niche partitioning strategies was hypothesized at others. Each locality is detailed and discussed by chronological order. The dietary categorization is based on previous studies on extant herbivores (microwear: [53,56,60,64]).

At **Gaimersheim (MP28)**, the median mesowear of *M. gaimersheimense* (2, $n = 4$) and the DMTA (low Str: high anisotropy) suggest a more abrasive diet than that of *R. romani*. The carbon isotopic content of the diet was also different between both species, but only two specimens of *M. gaimersheimense* were studied. Dietary preferences were clearly separated for the two rhinocerotids at Gaimersheim, with *M. gaimersheimense* being a mixed-feeder including tougher and harder objects than the browsing *R. romani*. In a previous study [84], Heissig compared *M. gaimersheimense* with *Diceros bicornis* (extant

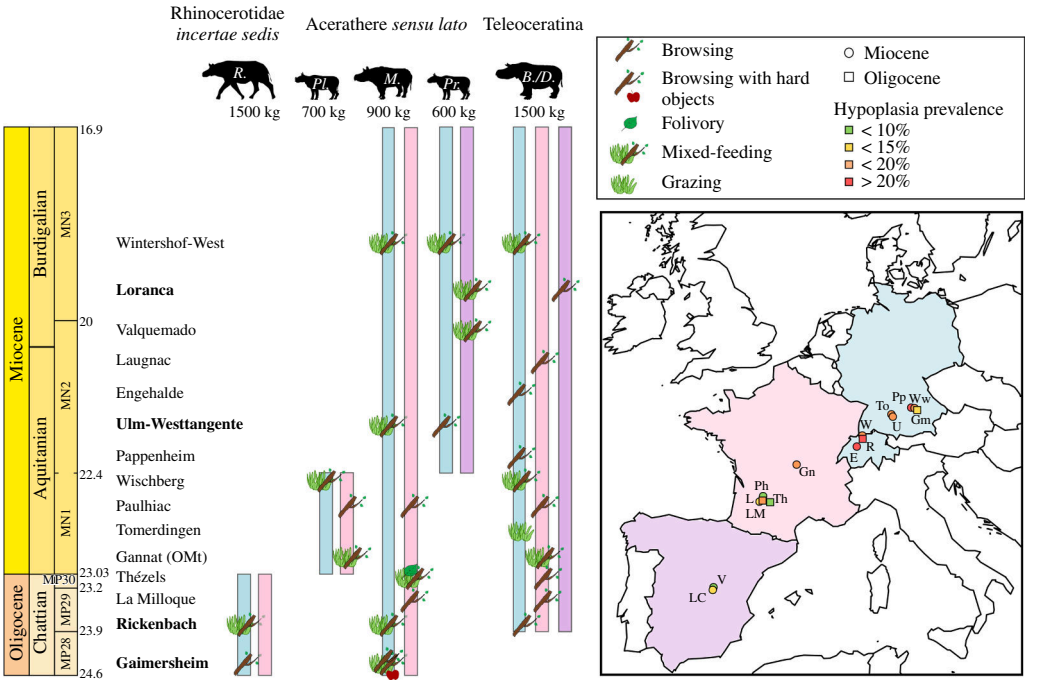

Figure 9. Spatio-temporal evolution of the palaeobiology and palaeoecology of the rhinocerotids during the Oligocene–Miocene transition. Distinct palaeoecological preferences at the localities in bold. Colour code by geographical provenance: blue, Central Europe (Germany and Switzerland); pink, Western Europe (France); and purple, Iberian Peninsula (Spain). Abbreviations in the silhouettes: R., *Ronzotherium*; Pl., *Pleuroceros*; M., *Mesaceratherium*; Pr., *Protaceratherium*; B./D., *Brachydiceratherium* / *Diaceratherium*. Abbreviations in the map: E, Engehalde (MN2); Gm, Gaimersheim (MP28); Gn, Gannat (MP30-MN1); L, Laugnac (MN2, reference); LC, Loranca del Campo (MN3a); LM, La Milloque (MP29); Ph, Paulhiac (MN1, reference); Pp, Pappenheim (MN2); R, Rickenbach (MP29, reference); To, Tomerdingen (MN1); Th, Thézels (MP30); U, Ulm-Westtangente (MN2a); V, Valquemado (MN2); W, Wischberg (MN1); and Ww, Wintershof-West (MN3).

black rhinoceros) based on tooth morphology, and proposed a similar generalist diverse and adaptable lifestyle, whereas for *R. romani* he only concluded that this species was not a steppe grazer. For the first comparison, *D. bicornis* has a similar body mass (800–1500 kg) [85], but a diet including more abrasive and hard objects, as suggested by mesowear scores [86] and DMT [60].

At **Rickenbach (MP29)**, both dental wear proxies suggested different feeding preferences, although not statistically significant (small sample). *Ronzotherium romani* had the highest median mesowear ruler score (4, $n = 3$), but low anisotropy (high Str values > 0.3). The high values of complexity and heterogeneity of the complexity suggest the inclusion of hard items and a certain variety in the diet, consistent with mixed-feeding. A previous study at Rickenbach inferred a short vegetation browsing diet for *R. romani* due to its low hypsodonty index (here HI = 1) and low head posture [87], but this would be more similar to the feeding behaviour of the species at Gaimersheim. *Brachydiceratherium lamilloquense* had the lowest median mesowear score (2, $n = 2$) consistent with the DMTA signature (high Str, medium Asfc and Hasfc) and pointing towards browsing habits. The low hypsodonty index (here 0.89, brachyodont) and the intermediate head posture were used in a previous study to infer high level browsing [87]. Eventually, the third species *M. gaimersheimense*, recognized in a recent revision [88], had a moderate median mesowear score (2, $n = 3$), high complexity (Asfc > 2) and low anisotropy (Str > 0.3) suggesting browsing.

At **La Milloque (MP29)**, both rhinocerotid species overlap for carbon isotopic content and DMT, although some slight differences can be noted. The mesowear median, however, highlights a higher abrasivity in the diet of *M. paulhiacense* (2, $n = 7$) compared with *B. lamilloquense* (1, $n = 5$). Both species appear to have been browsers, but probably fed on different plants or plant parts (different body mass, feeding height and mesowear). The study of the Moschidae species at La Milloque revealed very diverse dietary preferences, with the largest species in the range of extant grazers and smallest probably folivore [89]. These preferences are rather distinct from the ones inferred for the rhinocerotids here, which supports the conclusion of the authors of a relatively heterogeneous environment at the locality.

At **Thézels (MP30)**, the mesowear and isotopic content are only available for *M. gaimersheimense* and indicate browsing or mixed feeding. The DMTA, however, points towards a tough, abrasive diet (Str < 0.2). This pattern (low mesowear score, high anisotropy) has previously been linked to folivory [34,60], but could also be the result of C3 grazing or seasonal variations in the diet. C3 grazing has already been hypothesized for some brachyodont Moschidae at La Milloque based on their microwear [89]. Seasonality has previously been discussed at Thézels [90] and our results concur to a great aridity at this locality (see next section). Only one specimen of *B. lemanense* was examined for microwear and falls in the range of variation of *M. gaimersheimense*, suggesting at least a partial overlap in the dietary preferences of both species. Similar palaeoecologies have already been proposed for both rhinocerotids at Thézels: Blanchon *et al*. [91] interpreted them as browsers and cursorial forest dwellers. However, the body mass of these rhinocerotids is very different (850 kg for *M. gaimersheimense* and 1650 kg for *B. lemanense*), which could point to another strategy for niche partitioning.

At **Gannat (MP30 to MN1)**, dental wear (meso- and micro-wear) was studied for *B. lemanense* and *P. pleuroceros*, while isotopic content could only be retrieved for the first one. The median mesowear scores of both species are equal to 2, suggesting a potential overlap of the feeding preferences in the browser to mixed-feeder range. Only one specimen of *P. pleuroceros* could be studied for DMTA, and its signature is within the range of *B. lemanense* microwear, confirming the potential dietary overlap of both species.

Rhinocerotid material from the earliest Miocene (MN1) was scarce. At **Tomerdingen (MN1)**, only one species (*D. tomerdingense*) is recorded, for which only mesowear scoring was possible. The only molar examined had very high score suggesting grazing. At **Paulhiac (MN1)**, the median mesowear suggested soft browsing for both *Brachydiceratherium* species and the DMTA highlighted partial overlap between *B. lemanense* and all other species, notably for values of complexity. At **Wischberg (MN1)**, very few specimens could be analysed and do not allow for species comparison (only *Brachydiceratherium* for DMTA and only *P. pleuroceros* for mesowear), but both species are in the mixed-feeders range.

At **Pappenheim (MN2)**, there is only one species (*B. lemanense*), for which mesowear (2, $n = 1$) and DMTA (high Str, high Asfc, low HAsfc) suggest browsing. At **Ulm-Westtangente (MN2)**, there was a clear partitioning in the diet and/or habitat as highlighted by carbon isotopes and mesowear: *M. paulhiacense* had a more abrasive diet and was probably a mixed feeder, while *P. minutum* was a browser. The DMTA revealed less differences, as discussed by Hullot *et al*. [92]. At **Engehalde (MN2)**, very few specimens of rhinocerotids were found, limiting the analyses. The comparison between species was not possible, as the DMTA only includes one specimen of *B. aginense* (grinding facet only) and the mesowear was assessed only for *B. lemanense*. Both species are very similar and were probably browsers, in a humid wooded habitat close to steady rivers and swamp areas [93]. At **Laugnac (MN2)**, only one species was studied (*B. aginense*), for which low mesowear and DMT signature (high Str, moderate Asfc, low HAsfc) point towards soft browsing. At **Valquemado (MN2)**, only one species was found (*P. minutum*). The isotopes and DMTA suggest mixed-feeding habits, contrasting with the very low mesowear estimated on one specimen (0, $n = 1$).

At **Loranca del Campo (MN3)**, the mesowear and isotopic analysis only include the more abundant species: *P. minutum*. The DMT reveals different dietary preferences for both species (shearing facet): *P. minutum* has a higher anisotropy and slightly higher complexity, highlighting a tougher diet (mixed-feeder) than for *B.* aff. *aurelianense* (browser). The DMT of *P. minutum* between Valquemado and Loranca del Campo denotes a higher anisotropy at the latter (figure 7), consistent with morphological differences (size, gracility) and the more arid conditions previously inferred at Loranca [17]. These inferences are, however, not supported by our results, suggesting similar body mass (table 3) and similar environmental conditions at both localities (see next section). Eventually, at **Wintershof-West (MN3)**, the DMT of all three species overlaps in the mixed-feeding range. The mesowear of *B. aurelianense* (3, $n = 1$) and *M. paulhiacense* (1, $n = 1$) is, however, very distinct but the sample size is restricted.

4.2. Palaeoenvironmental conditions

The analyses of the isotopic content (carbon and oxygen) in the carbonates of the rhinocerotids's enamel allow for some palaeoenvironmental insights (table 4). However, these results are only partial, as the sample is limited to rhinocerotids at some localities, and should be completed by results on other taxa to provide more robust reconstructions. There was a clear shift towards higher values of $\delta^{13}C_{diet}$ for rhinocerotoids between La Milloque (MP29) and Thézels (MP30; figure 6). This suggests

Table 4. Reconstruction of the mean annual temperature (MAT) and precipitation (MAP) based on the isotopic content of the carbonates of the rhinocerotids' enamel.

	datation	MAT – Tütken *et al.* [47] (°C)	MAT – Skrzypek *et al.* [48] (°C)	MAP – Kohn [42] (without neg. values; mm yr^{-1})	MAP – Rey *et al.* [43] (mm yr^{-1})
Gaimersheim	MP28	13.6	12	273	857
Rickenbach	MP29	17.4	14.5	282	896
La Milloque	MP29	19.2	15.8	364	973
Thézels	MP30	19.8	16	95	460
Gannat	MP30-MN1	19.7	16.1	62	586
Ulm-Westtangente	MN2	15.6	13.4	317	637
Valquemado	MN2	20.6	16.5	72	513
Loranca del Campo	MN3	20.4	16.4	51	530

the establishment of more open and arid conditions during the latest Oligocene and persisting into the Early Miocene. MAT were rather warm at all localities but Gaimersheim, for which MAT was between 1.4 and 6°C lower than that at other localities (table 4). Regarding precipitation, the mean annual precipitation (MAP) suggests rather arid conditions at Thézels, Gannat, Valquemado and Loranca del Campo. The values estimated with Kohn's equation [42] are extremely low at these localities (less than 100 mm), and to a lesser extent for the whole dataset (less than 500 mm). This could be explained by the consumption of certain plants (for instance C4) [42], as well as the inclusion of altitude in this equation, which is difficult to estimate for fossil sites. Results for MAP are less drastic with Rey *et al.*'s equation [43], although the equation was built using the same dataset as Kohn [42]. In all cases, the palaeoenvironmental conditions seem relatively favourable at all localities investigated, consistent with the low (10%) to moderate (less than 20%) prevalence of hypoplasia for most rhinocerotids and localities (table 3; figure 5).

Our palaeoenvironmental insights can be confronted with the global climate predictions for the Late Oligocene–Early Miocene. The Late Oligocene Warming occurred between the MP26 and MP28 (approx. 26.5 to 24 Ma) [3], and was responsible for a temperature increase in terrestrial environments of up to 10°C [4,94,95]. Localities from our dataset all post-date this event, except maybe Gaimersheim (MP28), but the estimated MAT and MAP at this site suggest temperate conditions (table 4). Interestingly, localities from the MP29 (Rickenbach, La Milloque) and MP30 (Thézels) have warm MATs (greater than 15°C), suggesting the persistence of warm conditions during the latest Oligocene, at least locally. However, seasonal arid conditions have been hypothesized at Rickenbach, due to the presence of evaporite levels [38]. Interestingly, Rickenbach has one of the highest hypoplasia prevalence of the dataset (13/49; 26.53%), and notably *B. lamilloquense* (6/14; 42.86%) and *M. gaimersheimense* (6/13; 46.15%). Both teleoceratines and aceratheres *sensu lato* having been inferred as aquaphiles [96–98], which might explain the higher stress levels observed for these species compared with *R. romani* (1/21; 4.55%), supposedly more adapted to arid conditions [84]. Moreover, the Rickenbach level (reference of MP29) corresponds to the beginning of the 'Terminal Oligocene Crisis' [18] and a faunal turnover [11,87], which might have created stressful conditions for the rhinocerotids, notably through competition.

Moreover, the MAP estimates show a drastic drop between La Milloque and Thézels (table 4), indicating an increase in aridity during the MP30. Interestingly, the sediments at Thézels (tertiary limestone) and in the region (Quercy) suggest a seasonal aridity with periodic flooding [90]. Surprisingly, the hypoplasia prevalence at Thézels was one of the lowest in our dataset (11/171; 6.43%), although such conditions of periodic flooding have been linked with high hypoplasia prevalence in rhinocerotids at other sites [34,92]. The MP30 has been correlated to the interval between 23.2–23.03 Ma [5,6], which coincides with the drop in $\delta^{18}O_{\text{benthic foraminifera}}$ documenting the Mi−1 event [95]. Hence, this change in isotopic content could document the beginning of the Mi−1 glaciation event and associated vegetation changes. A few individuals from these two localities have been serially sampled to investigate seasonality. Most specimens display a sinusoidal variation of both $\delta^{13}C_{CO3}$

and $\delta^{18}O_{CO3}$ (electronic supplementary material, S2, figures 7 and 8), which could attest to some seasonality. Intra-individual variations observed for $\delta^{18}O_{CO3}$ (0.6 to 2.5‰, mostly around 1‰) were greater than that of $\delta^{13}C_{CO3}$ (0.2 to 2.4‰ but mostly around 0.5‰). Some teeth sampled (first and second molar, fourth premolars) might have recorded some weaning signal, but their variations are similar to that of third molars. We tested the correlation between the $\delta^{13}C$ and $\delta^{18}O$ values in the enamel carbonates, which would indicate a consistent influence of seasonal precipitation on the plants consumed. We only found one at La Milloque (rho = 0.5698249, S = 13273, *p*-value = 3.72×10^{-6}), most probably as more specimens were studied and with more samples per tooth.

Regarding Gannat, many discussions are found in the literature about dating problematics [99–101]. The presence of *R. romani* and *Eggysodon pomeli*, typical Oligocene taxa [70], would suggest an Oligocene age, whereas the other two species studied here (*P. pleuroceros* and *B. lemanense*) indicate early Miocene age. However, the specimens of *R. romani* and *E. pomeli* come from a different pit that is probably not contemporaneous. The isotopic content of the enamel of *B. lemanense* suggests rather warm and arid conditions that would be consistent with the installation of the warmer and more humid conditions of the Aquitanian, shortly after the Mi−1 event [2,7]. However, the conditions at Gannat are also very similar to that of Thézels, which could advocate for a latest Oligocene age. Hence, absolute dating appears crucial at Gannat, to untangle the situation. Two specimens were also serially sampled, one to detect a potential weaning signal (SpA) and one to investigate seasonality (SpB). Variations for $\delta^{18}O_{CO3}$ were greater than that of $\delta^{13}C_{CO3}$ in both specimens, similar to the results at La Milloque and Thézels (electronic supplementary material, S2, figures 4 to 6). Variations in the values of $\delta^{18}O_{CO3}$ in SpB are abrupt and might indicate a strong seasonality, although they are in the range of the weaning shift observed for SpA (electronic supplementary material, S2, figure 6).

In addition to the documentation of chronological aspects, the $\delta^{18}O$ values and estimated MATs might document geographical variations within Europe. Indeed, if localities are ordered spatially (Gaimersheim, Ulm-Westtangente, Rickenbach, Gannat, Thézels, La Milloque, Valquemado, Loranca del Campo; see figure 1, table 4 and electronic supplementary material, S2, figure 7), the MATs are increasing from northeast to southwest. This separates localities from Central (Germany, Switzerland) and Western Europe (France, Spain), with warmer and relatively drier conditions in the latter (except for La Milloque). Indeed, both localities of the Iberian peninsula, Valquemado and Loranca del Campo, had high MATs and low MAPs (table 4), consistent with previous findings indicating that this region was warmer and more arid than the rest of Europe already during the Early Miocene [78,102]. Interestingly, the DMTA also supports this, as specimens of *P. minutum* from both Iberian localities have slightly higher complexity and lower anisotropy (on the grinding facet) than at Ulm-Westtangente or Wischberg (figure 7). Regarding hypoplasia prevalence, rhinocerotids from Central European localities seem more affected, which does not reflect this potential aridity gradient.

The results of this study highlight several trends in the evolution of body mass, dietary preferences and susceptibility to stresses during the Oligocene–Miocene transition. Rhinocerotids in our dataset show a tendency of decreasing body mass during Late Oligocene, which is prolonged to the MN1 for some species (figure 8). During the Early Miocene, all trends (increase, stability, decrease) are observed depending on the species, contrary to what we expect (increase in body mass during the Early Miocene along with the appearance of mediportal forms). Interestingly, hypoplasia prevalence and body mass covaried, suggesting a higher stress susceptibility in bigger species. This result is not surprising, as bigger species are more vulnerable to environmental changes, as they have less babies, a longer gestation time, and they are more sensitive to habitat and population fragmentation [103,104]. However, other parameters might be responsible for this correlation, like a bigger size at localities with harsher conditions (Bergmann's rule: bigger species or population in colder climates [105]). This result, however, challenges the typical assumption that bigger species can buffer seasonality changes and tolerate lower nutritious diets [15], and shows that these stressful conditions also impact larger species.

The prevalence of hypoplasia is indeed greater around the Oligocene–Miocene limit (Gannat, Wischberg, Paulhiac) compared with Late Oligocene and Early Miocene where it oscillates between 5 and 15% for most species at most localities (table 3). This overall low to moderate prevalence is in line with our palaeoenvironmental insights (table 4), as well as with the warm and humid climate during the Aquitanian initiating the conditions of the Miocene Climatic Optimum [2]. Interestingly, Teleoceratine (here *Brachydiceratherium* and *Diaceratherium*) were the most affected taxa, recalling the pattern observed for *Brachypotherium* during the Early–Middle Miocene [106]. Teleoceratine have often been associated with humid environments and conditions [97,98], although a semi-aquatic lifestyle is not supported [107,108]. This water dependency might make these taxa more vulnerable to seasonality and

aridity. Sadly, the direct comparison with localities of the MN4 onward is difficult due to an important turnover in rhinocerotid species following the Proboscidean Datum Event [109], and marking the end of the Oligocene–Miocene transition [11].

5. Conclusions

The results of this study highlight several trends in the evolution of body mass, dietary preferences and susceptibility to stresses during the Oligocene–Miocene transition. Changes recorded in the enamel of rhinocerotids during this interval, suggest seasonal aridity at several localities (Thézels, Gannat, Valquemado and Loranca del Campo) and changes in the vegetation during the latest Oligocene. An increase in abrasivity is also observed in the DMT of several species during this interval, suggesting a shift in dietary preferences and/or habitats during the lastest Oligocene. The reconstructed palaeoenvironmental insights indicate favourable conditions, with warm mean annual temperatures (greater than 15°C) at most localities studied. This is consistent with the low to moderate prevalence of hypoplasia (5–20%). Even if all rhinocerotids were C3 feeders, with browsing to mixed-feeding preferences, we highlighted differences in dietary and or habitat preferences that could indicate niche partitioning at some localities (Gaimersheim, Ulm-Westtangente and Rickenbach). Our study showed great changes in the palaeoecology of the rhinocerotids during the Oligocene–Miocene transition, in line with taxonomic and morphological changes previously noted and with the global climatic and palaeoenvironmental changes at that time.

Ethics. This work did not require ethical approval from a human subject or animal welfare committee.

Data accessibility. All raw data are available in the electronic supplementary material [110].

Declaration of AI use. We have not used AI-assisted technologies in creating this article.

Authors' contributions. M.H.: conceptualization, data curation, formal analysis, funding acquisition, investigation, methodology, project administration, writing—original draft; C.M.: investigation, methodology, writing—review and editing; C.B.: methodology, validation, writing—review and editing; D.B.: conceptualization, validation, writing—review and editing; G.E.R.: conceptualization, funding acquisition, project administration, supervision, validation, writing—review and editing.

All authors gave final approval for publication and agreed to be held accountable for the work performed therein.

Conflict of interest declaration. We declare we have no competing interests.

Funding. The present work is part of a post doctoral project funded by a Research Fellowship of the Alexander von Humboldt Foundation (Germany). Two SYNTHESYS grants have also been obtained (FR-TAF_Call4_057, ES-TAF-TA4-781) and partly funded this work.

Acknowledgements. We are indebted to the curators and collection managers of the institutions that we visited: Eli Amson (SMNS Stuttgart), Susana Fraile Gracia (MNCN Madrid), Christine Argot and Guillaume Billet (MNHN Paris), Jérome Surault (University of Poitiers), Christophe Borrely (CECM Marseille), Ursula Menkveld (NHM Bern), Emmanuel Robert (University of Lyon), Didier Berthet and François Vigouroux (Musée des Confluences de Lyon), Loic Costeur and Florian Dammeyer (NHMB Basel), Jean-Marc Pouillon (Rhinopolis Gannat), Florence Lamera (Paleopolis Gannat) and Pia Geiger-Schütz and Peter Flückiger (Naturmuseum Ölten, Haus der Museen).

References

1. Costeur L, Legendre S. 2008 Spatial and temporal variation in European Neogene large mammals diversity. *Palaeogeogr. Palaeoclimatol. Palaeoecol.* **261**, 127–144. (doi:10.1016/j.palaeo.2008.01.011)
2. Westerhold T *et al*. 2020 An astronomically dated record of Earth's climate and its predictability over the last 66 million years. *Science* **369**, 1383–1387. (doi:10.1126/science.aba6853)
3. O'Brien CL, Huber M, Thomas E, Pagani M, Super JR, Elder LE, Hull PM. 2020 The enigma of Oligocene climate and global surface temperature evolution. *Proc. Natl Acad. Sci. USA* **117**, 25 302–25 309. (doi:10.1073/pnas.2003914117)
4. Mennecart B. 2015 The European ruminants during the '*Microbunodon* Event' (MP28, latest Oligocene): impact of climate changes and faunal event on the ruminant evolution. *PLoS One* **10**, e0116830. (doi:10.1371/journal.pone.0116830)
5. Solé F, Marandat B, Lihoreau F. 2020 The hyaenodonts (Mammalia) from the french locality of Aumelas (Hérault), with possible new representatives from the late Ypresian. *Geodiversitas* **42**, 185. (doi:10.5252/geodiversitas2020v42a13)
6. Speijer RP, Pälike H, Hollis CJ, Hooker JJ, Ogg JG. 2020 Chapter 28: the paleogene period. In *Geologic time scale 2020* (eds FM Gradstein, JG Ogg, MD Schmitz, GM Ogg), pp. 1087–1140. Amsterdam, The Netherlands: Elsevier. (doi:10.1016/B978-0-12-824360-2.00028-0)
7. Zachos JC, Shackleton NJ, Revenaugh JS, Pälike H, Flower BP. 2001 Climate response to orbital forcing across the Oligocene-Miocene boundary. *Science* **292**, 274–278. (doi:10.1126/science.1058288)

8. Pälike H, Norris RD, Herrle JO, Wilson PA, Coxall HK, Lear CH, Shackleton NJ, Tripati AK, Wade BS. 2006 The heartbeat of the Oligocene climate system. *Science* **314**, 1894–1898. (doi:10.1126/science.1133822)
9. Liebrand D, Lourens LJ, Hodell DA, de Boer B, van de Wal RSW, Pälike H. 2011 Antarctic ice sheet and oceanographic response to eccentricity forcing during the early Miocene. *Clim. Past* **7**, 869–880. (doi:10.5194/cp-7-869-2011)
10. Maridet O, Escarguel G, Costeur L, Mein P, Hugueney M, Legendre S. 2007 Small mammal (rodents and lagomorphs) European biogeography from the Late Oligocene to the mid Pliocene. *Glob. Ecol. Biogeogr.* **16**, 529–544. (doi:10.1111/j.1466-8238.2006.00306.x)
11. Scherler L, Mennecart B, Hiard F, Becker D. 2013 Evolutionary history of hoofed mammals during the Oligocene–Miocene transition in Western Europe. *Swiss J. Geosci.* **106**, 349–369. (doi:10.1007/s00015-013-0140-x)
12. Prothero DR, Guérin C, Manning E. 1989 The history of the Rhinocerotoidea. In *The evolution of perissodactyls* (eds DR Prothero, RM Schoch), pp. 322–340. New York, NY: Oxford University Press.
13. Kosintsev P *et al*. 2019 Evolution and extinction of the giant rhinoceros *Elasmotherium sibiricum* sheds light on late quaternary megafaunal extinctions. *Nat. Ecol. Evol.* **3**, 31–38. (doi:10.1038/s41559-018-0722-0)
14. Antoine PO, Becker D. 2013 A brief review of Agenian rhinocerotids in Western Europe. *Swiss J. Geosci.* **106**, 135–146. (doi:10.1007/s00015-013-0126-8)
15. Owen-Smith NR. 1988 *Megaherbivores: the influence of very large body size on ecology*. Cambridge, UK: Cambridge University Press.
16. Brunet M. 1979 Les Cricetidae (Rodentia, Mammalia) de La Milloque (bassin d'Aquitaine): horizon repère de l'Oligocène supérieur. *Geobios.* **12**, 653–673. (doi:10.1016/S0016-6995(79)80095-9)
17. Morales J *et al*. 1999 Vertebrados continentales del Terciario de la cuenca de Loranca (Provincia de Cuenca). *JCCM* 235–260.
18. Becker D, Bürgin T, Oberli U, Scherler L. 2009 *Diaceratherium lemanense* (Rhinocerotidae) from Eschenbach (Eastern Switzerland): systematics, palaeoecology, palaeobiogeography. *Neues Jahrb. Geol. Palaeontol.* **254**, 5–39. (doi:10.1127/0077-7749/2009/0002)
19. Blueweiss L, Fox H, Kudzma V, Nakashima D, Peters R, Sams S. 1978 Relationships between body size and some life history parameters. *Oecologia* **37**, 257–272. (doi:10.1007/BF00344996)
20. Brown JH, Gillooly JF, Allen AP, Savage VM, West GB. 2004 Toward a metabolic theory of ecology. *Ecology* **85**, 1771–1789. (doi:10.1890/03-9000)
21. Fortelius M, Damuth J, MacFadden BJ. 1990 Problems with using fossil teeth to estimate body sizes of extinct mammals. In *Body size in mammalian paleobiology: estimation and biological implications* (eds J Damuth, BJ MacFadden), pp. 207–228. Cambridge, UK: Cambridge University Press.
22. Millien V, Bovy H. 2010 When teeth and bones disagree: body mass estimation of a giant extinct rodent. *J. Mammal.* **91**, 11–18. (doi:10.1644/08-MAMM-A-347R1.1)
23. Janis CM. 1990 Correlation of cranial and dental variables with body size in ungulates and macropodoids. In *Body size in mammalian paleobiology: estimation and biological implications* (eds J Damuth, BJ MacFadden), pp. 255–300. Cambridge, UK: Cambridge University Press.
24. Legendre S. 1989 *Les communautés de mammifères du Paléogène (Eocène supérieur et Oligocène) d'Europe occidentale: structures, milieux et évolution*. München, Germany: Münchner Geowissenschaftliche Abhandlungen.
25. Damuth J. 1990 Problems in estimating body masses of archaic ungulates using dental measurements. In *Body size in mammalian paleobiology: estimation and biological implications* (eds J Damuth, BJ MacFadden), pp. 229–254. Cambridge, UK: Cambridge University Press.
26. Fortelius M, Kappelman J. 1993 The largest land mammal ever imagined. *Zool. J. Linn. Soc.* **108**, 85–101. (doi:10.1006/zjls.1993.1018)
27. Guatelli-Steinberg D. 2001 What can developmental defects of enamel reveal about physiological stress in nonhuman primates? *Evol. Anthropol.* **10**, 138–151. (doi:10.1002/evan.1027)
28. Mead AJ. 1999 Enamel hypoplasia in Miocene rhinoceroses (*Teleoceras*) from Nebraska: evidence of severe physiological stress. *J. Vertebr. Paleontol.* **19**, 391–397. (doi:10.1080/02724634.1999.10011150)
29. Upex B, Dobney K. 2012 Dental enamel hypoplasia as indicators of seasonal environmental and physiological impacts in modern sheep populations: a model for interpreting the zooarchaeological record. *J. Zool.* **287**, 259–268. (doi:10.1111/j.1469-7998.2012.00912.x)
30. Goodman AH, Rose JC. 1991 Dental enamel hypoplasias as indicators of nutritional status. In *Advances in dental anthropology* (eds M Kelley, C Larsen), pp. 279–293. New York, NY: Wiley-Liss.
31. Dobney K, Ervynck A. 2000 Interpreting developmental stress in archaeological pigs: the chronology of linear enamel hypoplasia. *J. Archaeol. Sci.* **27**, 597–607. (doi:10.1006/jasc.1999.0477)
32. Niven LB, Egeland CP, Todd LC. 2004 An inter-site comparison of enamel hypoplasia in bison: implications for paleoecology and modeling late plains archaic subsistence. *J. Archaeol. Sci.* **31**, 1783–1794. (doi:10.1016/j.jas.2004.06.001)
33. Hullot M, Antoine PO. 2022 Enamel hypoplasia on rhinocerotoid teeth: does CT-scan imaging detect the defects better than the naked eye? *Palaeovertebrata* **45**, e2. (doi:10.18563/pv.45.1.e2)
34. Hullot M, Laurent Y, Merceron G, Antoine PO. Paleoecology of the Rhinocerotidae (Mammalia, Perissodactyla) from Béon 1, Montréal-du-Gers (late early Miocene, SW France): insights from dental microwear texture analysis, mesowear, and enamel hypoplasia. *Palaeontol. Electron.* **24**, a27. (doi:10.26879/1163)
35. Stefaniak K *et al*. 2021 Browsers, grazers or mix-feeders? Study of the diet of extinct Pleistocene Eurasian forest rhinoceros *Stephanorhinus kirchbergensis* (Jäger, 1839) and woolly rhinoceros *Coelodonta antiquitatis* (Blumenbach, 1799). *Quat. Int.* **605–606**, 192–212. (doi:10.1016/j.quaint.2020.08.039)
36. Zanazzi A, Fletcher A, Peretto C, Thun Hohenstein U. 2022 Middle Pleistocene paleoclimate and paleoenvironment of Central Italy and their relationship with hominin migrations and evolution. *Quat. Int.* **619**, 12–29. (doi:10.1016/j.quaint.2022.01.011)

37. Bentaleb I *et al*. 2006 Rhinocerotid tooth enamel $^{18}O/^{16}O$ variability between 23 and 12 Ma in Southwestern France. *C. R. Geosci.* **338**, 172–179. (doi:10.1016/j.crte.2005.11.007)
38. Emery E, Tütken T, Becker D, Bucher S, Flückiger P, Berger JP. 2007 Rickenbach unter den Tropen... vor 25 Millionen Jahren! *N.G.S.O.* **40**, 51–64. https://www.e-periodica.ch/digbib/view?pid=ngs-004:2007:40::122#60
39. Cerling TE, Harris JM, Ambrose SH, Leakey MG, Solounias N. 1997 Dietary and environmental reconstruction with stable isotope analyses of herbivore tooth enamel from the Miocene locality of Fort Ternan, Kenya. *J. Hum. Evol.* **33**, 635–650. (doi:10.1006/jhev.1997.0151)
40. Tejada-Lara JV, MacFadden BJ, Bermudez L, Rojas G, Salas-Gismondi R, Flynn JJ. 2018 Body mass predicts isotope enrichment in herbivorous mammals. *Proc. R. Soc. B* **285**, 20181020. (doi:10.1098/rspb.2018.1020)
41. Tipple BJ, Meyers SR, Pagani M. 2010 Carbon isotope ratio of Cenozoic CO_2: a comparative evaluation of available geochemical proxies. *Paleoceanography* **25**. (doi:10.1029/2009PA001851)
42. Kohn MJ. 2010 Carbon isotope compositions of terrestrial C3 plants as indicators of (paleo)ecology and (paleo)climate. *Proc. Natl Acad. Sci. USA* **107**, 19 691–19 695. (doi:10.1073/pnas.1004933107)
43. Rey K, Amiot R, Lécuyer C, Koufos GD, Martineau F, Fourel F, Kostopoulos DS, Merceron G. 2013 Late Miocene climatic and environmental variations in Northern Greece inferred from stable isotope compositions ($\delta^{18}O$, $\delta^{13}C$) of equid teeth apatite. *Palaeogeogr. Palaeoclimatol. Palaeoecol.* **388**, 48–57. (doi:10.1016/j.palaeo.2013.07.021)
44. Coplen TB, Kendall C, Hopple J. 1983 Comparison of stable isotope reference samples. *Nature* **302**, 236–238. (doi:10.1038/302236a0)
45. Ayliffe LK, Lister AM, Chivas AR. 1992 The preservation of glacial-interglacial climatic signatures in the oxygen isotopes of elephant skeletal phosphate. *Palaeogeogr. Palaeoclimatol. Palaeoecol.* **99**, 179–191. (doi:10.1016/0031-0182(92)90014-V)
46. Lécuyer C *et al*. 2010 Oxygen isotope fractionation between apatite-bound carbonate and water determined from controlled experiments with synthetic apatites precipitated at 10–37°C. *Geochim. Cosmochim. Acta* **74**, 2072–2081. (doi:10.1016/j.gca.2009.12.024)
47. Tütken T, Vennemann TW, Janz H, Heizmann EPJ. 2006 Palaeoenvironment and palaeoclimate of the Middle Miocene lake in the Steinheim basin, SW Germany: a reconstruction from C, O, and Sr isotopes of fossil remains. *Palaeogeogr. Palaeoclimatol. Palaeoecol.* **241**, 457–491. (doi:10.1016/j.palaeo.2006.04.007)
48. Skrzypek G, Wiśniewski A, Grierson PF. 2011 How cold was it for Neanderthals moving to Central Europe during warm phases of the last glaciation? *Quat. Sci. Rev.* **30**, 481–487. (doi:10.1016/j.quascirev.2010.12.018)
49. Green JL, Croft DA. 2018 Using dental mesowear and microwear for dietary inference: a review of current techniques and applications. In *Methods in paleoecology* (eds DA Croft, DF Su, SW Simpson), pp. 53–73. Cham, Switzerland: Springer.
50. Ackermans NL. 2020 The history of mesowear: a review. *PeerJ* **8**, e8519. (doi:10.7717/peerj.8519)
51. Fortelius M, Solounias N. 2000 Functional characterization of ungulate molars using the abrasion-attrition wear gradient: a new method for reconstructing paleodiets. *Am. Mus. Nov.* **3301**, 1–36. (doi:10.1206/0003-0082(2000)301<0001:FCOUMU>2.0.CO;2)
52. Mihlbachler MC, Rivals F, Solounias N, Semprebon GM. 2011 Dietary change and evolution of horses in North America. *Science* **331**, 1178–1181. (doi:10.1126/science.1196166)
53. Jiménez-Manchón S, Blaise É, Albesso M, Gardeisen A, Rivals F. 2022 Quantitative dental mesowear analysis in domestic caprids: a new method to reconstruct management strategies. *J. Archaeol. Method Theory* **29**, 540–560. (doi:10.1007/s10816-021-09530-w)
54. Hillman-Smith AKK, Owen-Smith N, Anderson JL, Hall-Martin AJ, Selaladi JP. 1986 Age estimation of the White rhinoceros (*Ceratotherium simum*). *J. Zool.* **210**, 355–377. (doi:10.1111/j.1469-7998.1986.tb03639.x)
55. Taylor LA, Kaiser TM, Schwitzer C, Müller DWH, Codron D, Clauss M, Schulz E. 2013 Detecting inter-cusp and inter-tooth wear patterns in rhinocerotids. *PLoS One* **8**, e80921. (doi:10.1371/journal.pone.0080921)
56. Rivals F, Rabinovich R, Khalaily H, Valla F, Bridault A. 2020 Seasonality of the Final Natufian occupation at Eynan/Ain Mallaha (Israel): an approach combining dental ageing, mesowear and microwear. *Archaeol. Anthropol. Sci.* **12**, 1–15. (doi:10.1007/s12520-020-01190-3)
57. Winkler DE, Kaiser TM. 2011 A case study of seasonal, sexual and ontogenetic divergence in the feeding behaviour of the moose (*Alces alces* LINNÉ, 1758). *Abh. Naturwiss. Vereins. Hamburg.* **46**, 331–348.
58. Scott RS, Ungar PS, Bergstrom TS, Brown CA, Grine FE, Teaford MF, Walker A. 2005 Dental microwear texture analysis shows within-species diet variability in fossil hominins. *Nature* **436**, 693–695. (doi:10.1038/nature03822)
59. Francisco A, Blondel C, Brunetière N, Ramdarshan A, Merceron G. 2018 Enamel surface topography analysis for diet discrimination: a methodology to enhance and select discriminative parameters. *Surf. Topogr.* **6**, 015002. (doi:10.1088/2051-672X/aa9dd3)
60. Hullot M, Antoine PO, Ballatore M, Merceron G. 2019 Dental microwear textures and dietary preferences of extant rhinoceroses (Perissodactyla, Mammalia). *Mamm. Res.* **64**, 397–409. (doi:10.1007/s13364-019-00427-4)
61. Merceron G *et al*. 2016 Untangling the environmental from the dietary: dust does not matter. *Proc. R. Soc. B* **283**, 20161032. (doi:10.1098/rspb.2016.1032)
62. Scott RS, Ungar PS, Bergstrom TS, Brown CA, Childs BE, Teaford MF, Walker A. 2006 Dental microwear texture analysis: technical considerations. *J. Hum. Evol.* **51**, 339–349. (doi:10.1016/j.jhevol.2006.04.006)
63. Calandra I, Bob K, Merceron G, Blateyron F, Hildebrandt A, Schulz-Kornas E, Souron A, Winkler DE. 2022 Surface texture analysis in Toothfrax and MountainsMap® SSFA module: different software packages, different results? *Peer. Community. J.* **2**, e77. (doi:10.24072/pcjournal.204)
64. Scott JR. 2012 Dental microwear texture analysis of extant African Bovidae. *Mammalia* **76**, 157–174. (doi:10.1515/mammalia-2011-0083)
65. Talamoni SA, Assis MAC. Feeding habit of the Brazilian tapir, *Tapirus terrestris* (Perissodactyla: Tapiridae) in a vegetation transition zone in south-eastern Brazil. *Zoologia* **26**, 251–254. (doi:10.1590/S1984-46702009000200007)
66. Wickham H. 2016 *ggplot2: elegant graphics for data analysis*. New York, NY: Springer-Verlag.

67. Wilke CO. 2020 *cowplot: streamlined plot theme and plot annotations for 'ggplot2'*. R package version 1.1.0. See https://CRAN.R-project.org/package=cowplot.
68. Auguie B. 2017 *gridExtra: miscellaneous functions for 'grid' graphics*. R package version 2. 3. See https://CRAN.R-project.org/package=gridExtra.
69. Wasserstein RL, Lazar NA. 2016 The ASA statement on *p*-values: context, process, and purpose. *Am. Stat.* **70**, 129–133. (doi:10.1080/00031305.2016.1154108)
70. Tissier J, Antoine PO, Becker D. 2021 New species, revision, and phylogeny of *Ronzotherium* Aymard, 1854 (Perissodactyla, Rhinocerotidae). *Eur. J. Taxon.* **753**, 1–80. (doi:10.5852/ejt.2021.753.1389)
71. Jame C, Tissier J, Maridet O, Becker D. 2019 Early agenian rhinocerotids from Wischberg (Canton Bern, Switzerland) and clarification of the systematics of the genus *Diaceratherium*. *PeerJ* **7**, e7517. (doi:10.7717/peerj.7517)
72. Tissier J, Antoine PO, Becker D. 2020 New material of *Epiaceratherium* and a new species of *Mesaceratherium* clear up the phylogeny of early Rhinocerotidae (Perissodactyla). *R. Soc. Open Sci.* **7**, 200633. (doi:10.1098/rsos.200633)
73. Sizov A, Klementiev A, Antoine PO. 2023 An early miocene skeleton of *Brachydiceratherium* lavocat, 1951 (mammalia, perissodactyla) from the baikal area, russia, and a revised phylogeny of eurasian teleoceratines. *Paleontology*. (doi:10.1101/2022.07.06.498987)
74. Domingo L, Koch PL, Hernández Fernández M, Fox DL, Domingo MS, Alberdi MT. 2013 Late Neogene and early Quaternary paleoenvironmental and paleoclimatic conditions in Southwestern Europe: isotopic analyses on mammalian taxa. *PLoS One* **8**, e63739. (doi:10.1371/journal.pone.0063739)
75. Urban MA, Nelson DM, Jimenez-Moreno G, Chateauneuf JJ, Pearson A, Hu FS. 2010 Isotopic evidence of C_4 grasses in southwestern Europe during the Early Oligocene–Middle Miocene. *Geology* **38**, 1091–1094. (doi:10.1130/G31117.1)
76. Strömberg CA. 2011 Evolution of grasses and grassland ecosystems. *Annu. Rev. Earth Planet. Sci.* **39**, 517–544. (doi:10.1146/annurev-earth-040809-152402)
77. Urban MA, Nelson DM, Jiménez-Moreno G, Hu FS. 2016 Carbon isotope analyses reveal relatively high abundance of C_4 grasses during early–middle Miocene in southwestern Europe. *Palaeogeogr. Palaeoclimatol. Palaeoecol.* **443**, 10–17. (doi:10.1016/j.palaeo.2015.11.012)
78. Saarinen J, Mantzouka D, Sakala J. 2020 Aridity, cooling, open vegetation, and the evolution of plants and animals during the Cenozoic. In *Nature through time: virtual field trips through the nature of the past* (eds E Martinetto, E Tschopp, RA Gastaldo), pp. 83–107. Cham, Switzerland: Springer International Publishing. (doi:10.1007/978-3-030-35058-1_3)
79. Barbehenn RV, Chen Z, Karowe DN, Spickard A. 2004 C_3 grasses have higher nutritional quality than C_4 grasses under ambient and elevated atmospheric CO_2. *Glo. Change Biol.* **10**, 1565–1575. (doi:10.1111/j.1365-2486.2004.00833.x)
80. Mihlbachler MC, Solounias N. 2002 Body size, dental microwear, and brontothere diets through the Eocene. *J. Vertebr. Paleontol.* **22**, 88A.
81. Saarinen J, Eronen J, Fortelius M, Seppä H, Lister AM. 2016 Patterns of diet and body mass of large ungulates from the pleistocene of Western Europe, and their relation to vegetation. *Palaeontol. Electron.* **19**, 1–58. (doi:10.26879/443)
82. Orlandi-Oliveras G, Köhler M, Clavel J, Scott R, Mayda S, Kaya T, Merceron G. 2022 Feeding strategies of circum-Mediterranean hipparionins during the late Miocene: exploring dietary preferences related to size through dental microwear analysis. *Palaeontol. Electron.* **25**, 1–45. (doi:10.26879/990)
83. Steuer P, Südekum KH, Tütken T, Müller DWH, Kaandorp J, Bucher M, Clauss M, Hummel J. 2014 Does body mass convey a digestive advantage for large herbivores? *Funct. Ecol.* **28**, 1127–1134. (doi:10.1111/1365-2435.12275)
84. Heissig K. 1969 Die Rhinocerotidae (Mammalia) aus der oberoligozänen Spaltenfüllung von Gaimersheim bei Ingolstadt in Bayern und ihre phylogenetische Stellung. *Abh. Bayer. Akad. Wiss., Math.-Nat.wiss. Kl.* **138**, 1–133.
85. Hillman-Smith AKK, Groves CP. 1994 *Diceros bicornis*. *Mamm. Species* **455**, 1. (doi:10.2307/3504292)
86. Mihlbachler MC, Campbell D, Chen C, Ayoub M, Kaur P. 2018 Microwear–mesowear congruence and mortality bias in rhinoceros mass-death assemblages. *Paleobiology* **44**, 131–154. (doi:10.1017/pab.2017.13)
87. Mennecart B, Scherler L, Hiard F, Becker D, Berger JP. 2012 Large mammals from Rickenbach (Switzerland, reference locality MP29, Late Oligocene): biostratigraphic and palaeoenvironmental implications. *Swiss J. Palaeontol.* **131**, 161–181. (doi:10.1007/s13358-011-0031-6)
88. Tissier J, Geiger-Schütz P, Flückiger PF, Becker D. 2021 Neue Erkenntnisse über die Nashorn-Funde von Rickenbach (SO) (Oberes Oligozän, Kanton Solothurn, Schweiz) aus der Sammlung des Naturmuseums Olten. *NGSO* **44**, 25–51. (doi:10.5169/seals-904323)
89. Novello A, Blondel C, Brunet M. 2010 Feeding behavior and ecology of the Late Oligocene Moschidae (Mammalia, Ruminantia) from La Milloque (France): evidence from dental microwear analysis. *Compt. Rend. Palevol.* **9**, 471–478. (doi:10.1016/j.crpv.2010.10.001)
90. de Bonis L, Guinot Y. 1987 Le gisement de Vertébrés de Thézels (Lot) et la limite Oligo-Miocene dans les formations continentales du bassin d'Aquitaine. *Münchn. Geowiss. Abh.* **10**, 49–58.
91. Blanchon M, Antoine PO, Blondel C, de Bonis L. 2018 Rhinocerotidae (Mammalia, Perissodactyla) from the latest Oligocene Thézels locality, SW France, with a special emphasis on *Mesaceratherium gaimersheimense* Heissig, 1969. *Ann. Paléontol.* **104**, 217–229. (doi:10.1016/j.annpal.2018.06.001)
92. Hullot M, Martin C, Blondel C, Rössner GE. 2024 Life in a Central European warm-temperate to subtropical open forest: paleoecology of the rhinocerotids from Ulm-Westtangente (Aquitanian, Early Miocene, Germany). *Sci. Nat.* **111**, 10. (doi:10.1007/s00114-024-01893-w)
93. Becker D, Antoine PO, Engesser B, Hiard F, Hostettler B, Menkveld-Gfeller U, Mennecart B, Scherler L, Berger JP. 2010 Late Aquitanian mammals from Engehalde (Molasse Basin, Canton Bern, Switzerland). *Ann. Paléontol.* **96**, 95–116. (doi:10.1016/j.annpal.2011.03.001)
94. Vianey-Liaud M. 1991 Les rongeurs de l'Eocène terminal et de l'Oligocène d'Europe comme indicateurs de leur environnement. *Palaeogeogr. Palaeoclimatol. Palaeoecol.* **85**, 15–28. (doi:10.1016/0031-0182(91)90023-K)

95. Zachos J, Pagani M, Sloan L, Thomas E, Billups K. 2001 Trends, rhythms, and aberrations in global climate 65 Ma to present. *Science* **292**, 686–693. (doi:10.1126/science.1059412)
96. Guérin C. 1980 *Les rhinocéros (Mammalia, Perissodactyla) du Miocène terminal au Pleistocène supérieur en Europe occidentale: comparaison avec les espèces actuelles*. Villeurbanne, France: Documents de l'Université de Lyon.
97. Cerdeño E. 1998 Diversity and evolutionary trends of the family Rhinocerotidae (Perissodactyla). *Palaeogeogr. Palaeoclimatol. Palaeoecol.* **141**, 13–34. (doi:10.1016/S0031-0182(98)00003-0)
98. Prothero DR. 1998 Rhinocerotidae. *Evolution of the tertiary mammals of North America*, pp. 595–605. Cambridge, UK: Cambridge University Press.
99. Hugueney M. 1997 Biochronologie mammalienne dans le Paléogène et le Miocène inférieur du Centre de la France: synthèse réactualisée. In *Actes du Congrès BiochroM'97, 21. MéM. Trav. E.P.H.E. Inst., Montpellier*, pp. 417–430.
100. Boada-Sana A, Hervet S, Antoine PO. 2007 Nouvelles données sur les rhinoceros fossiles de Gannat (Allier, limite Oligocene-Miocene). *Rev. Sci. Nat. Auvergne* **71**, 3–25.
101. Hugueney M, Mein P, Maridet O. 2012 Revision and new data on the early and middle Miocene soricids (Soricomorpha, Mammalia) from Central and South-Eastern France. *Swiss J. Palaeontol.* **131**, 23–49. (doi:10.1007/s13358-011-0036-1)
102. Fortelius M, Eronen JT, Kaya F, Tang H, Raia P, Puolamäki K. 2014 Evolution of Neogene mammals in Eurasia: environmental forcing and biotic interactions. *Annu. Rev. Earth Planet. Sci.* **42**, 579–604. (doi:10.1146/annurev-earth-050212-124030)
103. Cardillo M, Mace GM, Jones KE, Bielby J, Bininda-Emonds ORP, Sechrest W, Orme CDL, Purvis A. 2005 Multiple causes of high extinction risk in large mammal species. *Science* **309**, 1239–1241. (doi:10.1126/science.1116030)
104. González-Suárez M, Gómez A, Revilla E. 2013 Which intrinsic traits predict vulnerability to extinction depends on the actual threatening processes. *Ecosphere* **4**, 1–16. (doi:10.1890/ES12-00380.1)
105. Blackburn TM, Gaston KJ, Loder N. 1999 Geographic gradients in body size: a clarification of Bergmann's rule. *Divers. Distrib.* **5**, 165–174. (doi:10.1046/j.1472-4642.1999.00046.x)
106. Hullot M, Merceron G, Antoine PO. 2023 Spatio-temporal diversity of dietary preferences and stress sensibilities of early and middle Miocene rhinocerotidae from Eurasia: impact of climate changes. *Peer Community J.* **3**, article (doi:10.24072/pcjournal.222)
107. Clementz MT, Holroyd PA, Koch PL. 2008 Identifying aquatic habits of herbivorous mammals through stable isotope analysis. *Palaios* **23**, 574–585. (doi:10.2110/palo.2007.p07-054r)
108. Wang B, Secord R. 2020 Paleoecology of *Aphelops* and *Teleoceras* (Rhinocerotidae) through an interval of changing climate and vegetation in the Neogene of the Great Plains, Central United States. *Palaeogeogr. Palaeoclimatol. Palaeoecol.* **542**, 109411. (doi:10.1016/j.palaeo.2019.109411)
109. Tassy P. 1990 The 'Proboscidean Datum Event:' how many proboscideans and how many events? In *European neogene mammal chronology* (eds EH Lindsay, V Fahlbusch, P Mein), pp. 237–252. New York, NY: Springer.
110. Hullot M, Martin C, Blondel C, Becker D, Rössner GE. 2024 Data from: Evolutionary paleoecology of European rhinocerotids across the Oligocene-Miocene transition. Figshare. (doi:10.6084/m9.figshare.c.7477982)